

Contents lists available at ScienceDirect

Algal Research

journal homepage: www.elsevier.com/locate/algal





Moving horizon estimation in microalgae-bacteria based wastewater treatment using online and analytical multi-rate measurements

Irina Bausa-Ortiz ^{a,b,*}, Erika Oliveira-Silva ^{a,b}, Raúl Muñoz ^{b,c}, Smaranda P. Cristea ^{a,b}, Cesar de Prada ^{a,b}

- ^a Institute of Sustainable Processes, Paseo Prado de la Magdalena 3-5, Valladolid, 47011, Spain
- b Department of Systems Engineering and Automatic Control, University of Valladolid, Paseo Prado de la Magdalena 3-5, Valladolid, 47011, Spain
- c Department of Chemical Engineering and Environmental Technology, University of Valladolid, Real de Burgos s/n, Valladolid, 47011, Spain

ARTICLE INFO

Keywords: microalgae moving horizon estimation photobioreactor software sensors state estimation wastewater treatment

ABSTRACT

Population growth and industrialization have resulted into a substantial increase in wastewater production. thereby establishing water purification as a primary concern on a global scale. In this context, microalgaebacteria based wastewater treatment has emerged as a solution for wastewater treatment and nutrient recovery at a low-energy demand. Nevertheless, operation of this type of wastewater treatment plants is more complex and requires of advanced control systems, capable of maintaining its key variables within appropriate ranges in spite of the periodic variations in environmental variables and wastewater composition. Very often, the implementation of state feedback control laws and model-based control techniques in these processes necessitates full information of the states and other variables of the system in real-time. However, in practical scenarios, only a subset of the variables of microalgae-bacteria processes can be measured online due to the need for more reliable measuring devices or the high costs of online sensors. In addition, these biological processes are subjected to frequent variations, so that the parameters of the models representing them requires continuous adaptation. This paper presents the application of a moving horizon estimation technique to a wastewater treatment process with microalgae and bacteria. The objective of this study is to estimate those variables or parameters that cannot be measured reliably online. This process was nonlinear and subject to uncertainties in the states and parameters. The estimation was coded using MATLAB® software, and simulation results demonstrated the effectiveness of estimation in this biological process, characterized by the availability of multi-rate measurements.

1. Introduction

The utilization of microalgae as a wastewater treatment technology has emerged as a promising and sustainable solution, with the potential to address the high energy costs and loss of resources associated with mechanical aeration in conventional wastewater treatment methods [1]. Domestic and industrial wastewaters, which are characterized by high carbon, nitrogen, and phosphorus concentrations, require treatment prior to discharge into natural water bodies to prevent oxygen depletion, toxicity issues, and eutrophication. The capacity of microalgae to concurrently remove carbon, nitrogen, and phosphorus via mixotrophic assimilation confers a substantial advantage over conventional wastewater treatment technologies, such as aerobic activated sludge or anaerobic digestion, which are limited in their ability to recover nutrients. The potential for further utilization of the harvested microalgae

biomass to produce biofertilizers, biofuels, and other bioproducts renders this technology an attractive alternative for cost-effective wastewater treatment and nutrient management [2,3].

Despite the long-standing research in this field, these systems have only recently undergone improvements to meet industry demands and effluent quality regulations. In the context of large-scale microalgae-bacteria systems, novel techniques from biotechnology and control engineering must be applied to ensure the robustness, durability, and optimized operation of these processes. Mathematical models, control strategies, state estimation techniques, and process optimization techniques are important tools to operate properly these complex systems but need to be re-examined and adapted to the context of multiple perturbations and evolving environmental conditions that affect these

Mathematical models are at the core of numerous contemporary

^{*} Corresponding author at: Institute of Sustainable Processes, Paseo Prado de la Magdalena 3-5, Valladolid, 47011, Spain. *E-mail address:* irina.bausa@uva.es (I. Bausa-Ortiz).

methodologies aimed at enhancing the comprehension of biological processes and facilitating their operation. In the context of plant operation, advanced control strategies have emerged as promising instruments to enhance the performance of microalgae production systems, particularly within the context of large-scale cultivation plants [4]. The implementation of state feedback control laws and model-based control techniques, such as Model Predictive Control (MPC), necessitates complete online information of the system. However, in practical scenarios, only a subset of the states or key variables of microalgae-bacteria processes can be measured due to the necessity for more reliable measuring devices or the high cost of on-line sensors [5].

The basic hardware instrumentation in microalgae-bacteria-based wastewater treatment plants typically provides online measurements of temperature, pH, dissolved oxygen, and flow rate. However, this is not the case for other component concentrations (biomass, substrates, and metabolites), which are crucial for understanding the system state. Despite of the significant progress in the field, many current hardware sensors for concentration measurement still exhibit significant drawbacks, including expensive probes, discrete-time measurements, and offline solutions, among others. Consequently, state estimators (often termed software sensors) emerge as a promising alternative to determine the non-measurable states and concurrently reduce the utilization of costly sensors.

State estimators employ a dynamic model of the process, knowledge about the process inputs, and the availability of hardware sensors to measure certain variables to estimate those difficult to measure. In addition, as these biological processes are subjected to frequent variations in environmental parameters and wastewater characteristics, the parameters of the models representing them require continuous adaptation. State estimators are also able to include these parameters among the variables being estimated.

The diversity of state estimation techniques arising from intrinsic differences in chemical process systems underscores the importance of selecting the proper technique for design and implementation in specific applications. The seminal contributions of Luenberger [6–9] and Kalman [10,11] in the 1960s laid the foundation for the development of state observers and Kalman Filter (KF)-based estimators. However, over the years, research in the design of state estimators has become increasingly popular yet challenging due to the requirements of high accuracy, low cost, and good prediction performances.

In the context of bioprocesses, the estimator design problem is particularly challenging. In addition to the scarcity of online measurements, additional challenges are presented by considerable nonlinear dynamics governing the cultivation process and the consequent modeling complexity. The KF-based estimators are the most widely applied [4,12,13]. The current state of the art of KF-based estimators in microalgae processes includes various reports of estimators applied together with control and optimization techniques due to the necessity of the entire state vector for system monitoring and control [4,13,14]. These estimators present satisfactory results, provided that linear approximation remains valid, the signal has low noise, and constraints are negligible.

Another approach for nonlinear systems that has gained popularity over the past two decades among researchers and industrial practitioners of MPC is the Moving Horizon Estimation (MHE) approach [15–17]. This approach formulates the state estimation problem as an optimization problem over a moving time window, akin to the MPC formulation. The strategy of MHE has been demonstrated to exhibit numerous advantages over other nonlinear state estimation techniques. It has the capacity to incorporate a priori process knowledge by including constraints on the estimated states and disturbances. Furthermore, its performance is frequently superior because nonlinear model equations can be used directly without the necessity of linearization. A salient benefit of this approach is its capacity to generate both filtered and smoothed estimates of states within the same window. Furthermore, MHE has the capacity to estimate states, parameters, and

model-plant mismatch concurrently. The capacity to assess model-plant discrepancy is essential for compensating for errors or simplifications in the model. MHE has been demonstrated to be applicable in bioprocesses [18–20], including the state estimation in conventional wastewater treatment plants [21–23]. In the context of microalgae-based processes, the application of MHE is restricted to a limited number of research works [24], and, to the best of the authors' knowledge, there are not publications addressing domestic wastewater treatment plants based on microalgae-bacteria consortia. Despite its potential, MHE has not been extensively explored in this area.

The inherent nonlinear characteristics of microalgae-based wastewater treatment processes, coupled with the operational constraints associated with these processes, underscore the viability of MHE as a solution to the state estimation problem in this context. This assertion is further supported by previous experience in applying MHE to other biological and conventional wastewater treatment processes. The aim of this study is to propose an MHE strategy for state and parameter estimation in an industrial microalgae-based wastewater treatment plant. The online state estimation would pave the way for the future implementation of control and optimization strategies in the plant based on the actual values of the states. This objective is particularly challenging in such processes, where some states are measured offline and depend on analytical procedures that are highly time and resource consuming.

2. Materials and methods

2.1. Moving horizon estimation

MHE is a powerful tool for state estimation in dynamic systems, transforming the problem into an optimization problem. This approach searches for the states and parameters that minimize the discrepancy between measured and model-predicted outputs over a sliding window of past data. Additionally, MHE effectively incorporates unmeasured disturbances and other inaccuracies within this finite sequence of past measurements, and consider the admissible ranges of the different variables involved.

Unlike filter-based approaches for nonlinear systems such as the Extended Kalman Filter (EKF), MHE offers greater flexibility in handling constraints and system nonlinearities. The ability to incorporate additional constraints on estimated variables allows for enforcing physical limitations, integrating valuable information about the system's characteristics (such as ensuring concentrations remain positive or molar fractions stay within the [0,1] range). These constraints not only improve the physical realism of the estimates but also enhance the efficiency of the optimization solver by reducing the search space. As a result, estimation errors decrease, as more information is utilized in the optimization process.

It is important to acknowledge that nonlinear optimization with constraints increases computational complexity. However, with recent advancements in computing power and improved nonlinear solvers, MHE has become more practical, allowing solutions to be obtained within a reasonable timeframe. In highly nonlinear systems, such as biological processes, MHE typically outperforms EKF, which relies on the assumption that the system behaves linearly during updates, a condition that may not always hold.

Another key advantage of MHE is its versatility in scenarios where plant measurements are available at different frequencies (e.g. measurements from plant transmitters and from the lab). Traditional state estimation methods often assume that all relevant states can be observed from high-frequency measurements, but this is not always the case. Some states may only be inferred from less frequent measurements, making multi-rate measurements essential. By incorporating slower measurements into the estimation process, MHE improves both the quality of state estimates and the overall observability of the system, addressing potential information gaps.

The MHE dynamic optimization problem can be defined as problem

(1)–(7) below and Fig. 1. The problem is solved at regular time intervals or sampling times k. At current time k, the estimation considers a past horizon $t \in [t_{k-n_e}, t_k]$, where n_e represents the number of past sampling time included in the estimation. Within this horizon, the inputs u_{k-i} to the process over the intervals $[t_{k-i}, t_{k-i+1}]$, and the process measurements collected at t_{k-i} , denoted as $y_{P,k-i}$, are known for $i=1,\ldots,n_e$. The past horizon of the MHE is illustrated in Fig. 1.

The decision variables in this problem include the state values at the beginning of the sliding window of past data (\mathbf{x}_{k-n_e}) , and the past unmeasured system disturbances, unknown parameters, or system noise accounting for modeling errors (and unknown dynamics) (\mathbf{w}_{k-i}) . The objective (1) is to minimize discrepancies between the model-predicted outputs (\mathbf{y}_k) and the measured values $(\mathbf{y}_{P,k})$, while also considering the deviation between the newly estimated past initial state \mathbf{x}_{k-n_e} and the state estimated from the previous MHE execution at time $t-n_e$ $(\widehat{\mathbf{x}}_{k-n_e})$, as well as maintaining consistency or minimizing the past disturbances (or parameters $\mathbf{\theta}_{k-i}$) and \mathbf{w}_{k-i} . Then, the trajectory of the state variables up to time k $[\mathbf{x}_{k-n_e},...,\mathbf{x}_k]$ is estimated using the process model. The name *moving horizon* estimation is derived from this problem formulation: at each sampling time t_k , a new measurement $\mathbf{y}_{P,k-n_e-1}$ is discarded from the estimation window.

The weighting matrices Q_y , Q_x and Q_w regulate the influence of each term on the cost function. The optimization problem is subjected to the dynamic system model (2) and (3), as well as the operational and physical constraints defined in (4). The problem also incorporates inequality constraints (5) to restrict disturbances to the permissible range. The incorporation of additional constraints in the values of the states (6) and parameters (7) could enhance the estimation performance.

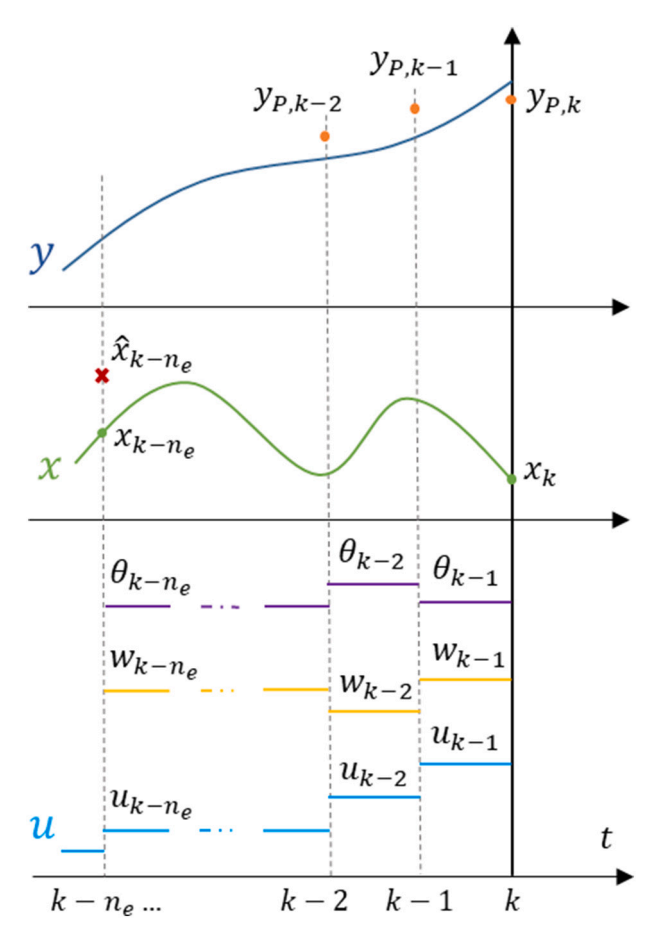


Fig. 1. Past values for the MHE estimation.

$$\min_{\substack{x_{k-n_e} | w_{k-i} \theta_{k-i} \\ i=1,\dots,n_e}} \sum_{i=0}^{n_e-1} \left\| y_{k-i} - y_{P,k-i} \right\|_{\boldsymbol{Q_y}}^2 + \left\| x_{k-n_e} - \widehat{\boldsymbol{x}}_{k-n_e} \right\|_{\boldsymbol{Q_x}}^2 + \sum_{i=1}^{n_e} \left\| w_{k-i} \right\|_{\boldsymbol{Q_w}}^2$$

(1)

$$s.t.f(\dot{x}, x, u, w, \theta) = 0, \forall t \in [t_{k-n_e}, t_k], x(t_{k-n_e}) = x_{k-n_e}$$
 (2)

$$h(\mathbf{x}, \mathbf{u}, \mathbf{y}, \mathbf{w}, \boldsymbol{\theta}) = 0, \forall t \in [t_{k-n_e}, t_k]$$
(3)

$$g(\boldsymbol{u},\boldsymbol{y}) \le 0, \forall t \in [t_{k-n_{\star}}, t_{k}] \tag{4}$$

$$\mathbf{w}^{L} \le w_{k-i} \le \mathbf{w}^{U}, i = 1...n_{e} \tag{5}$$

$$\mathbf{x}^{L} \leq \mathbf{x}_{k-i} \leq \mathbf{x}^{U}, i = 1...n_{e} \tag{6}$$

$$\boldsymbol{\theta}^{L} < \theta_{k-i} < \boldsymbol{\theta}^{U}, i = 1...n_{o} \tag{7}$$

This is a dynamic optimization problem that can be solved either with a sequential approach involving a dynamic simulator and a non-linear optimizer or directly with a non-linear solver after full discretization. The structure of the MHE algorithm is summarized in Fig. 2.

State estimation employing the MHE technique is also beneficial in scenarios where plant measurements are not available at the same frequency. This situation is illustrated in Fig. 3, where the measurements of outputs y_1 and y_2 (represented with circles), are available with a sampling period greater than the sampling period of the measurements of the output y_3 . The prevailing state estimation methodologies typically utilize solely the rapid measurements ($y_{3P,k}$ in Fig. 3), operating under the assumption that all states of interest are observable from them. However, this assumption does not always hold true, and there exist instances where states cannot be observed from the rapid measurements alone. Consequently, the utilization of measurements obtained at varying rates has the potential to enhance the observability properties of the system. Therefore, it is recommended to use methodologies capable of managing multi-rate measurements, with the objective of leveraging the slower measurements to enhance the quality of state estimates or their observability.

2.2. Plant description

This study considers a hypothetical wastewater treatment plant (WWTP) for a population of approximately 5000 inhabitants, treating an average flow rate of 875 m³/d. The system consists of two parallel High-Rate Algal Ponds (HRAPs), each with an area of 10,208 m², designed in the typical form of raceways with two channels and two reversals (452 m long and 22.6 m wide). The HRAPs have a depth of 0.3 m and operate at a Hydraulic Retention Time (HRT) of 7 days. Two settlers, each with a total working volume of 293.75 m³, are connected to the output of each HRAP. The algal-bacterial biomass settled is recirculated to the HRAP to enhance nutrient assimilation and biomass settling ability. It is hypothesized that the algal-bacterial WWTP is preceded by a pre-treatment stage with primary sedimentation to remove the solid fraction of the wastewater. The schematic representation of the plant is depicted in Fig. 4, and the average composition of the inlet domestic wastewater is listed in Table 1. The values for wastewater composition were obtained from the typical domestic wastewater concentrations reported in [25.26].

The algal bacterial broth is composed of a consortium of microalgae and bacteria. The microalgae consortia consist of different strains utilized for wastewater treatment. The bacterial groups encompass heterotrophic bacteria and autotrophic bacteria (ammonium-oxidizing bacteria and nitrite-oxidizing bacteria). It is hypothesized that HRAPs are inoculated with 2.5 gVSS/L of microalgae consortia and 2.5 gVSS/L of activated sludge. The particulate components' relative proportions in the sludge are assumed based on those proposed in the Activated Sludge Model 2 (ASM2) [26]. The concentration of particulate components in

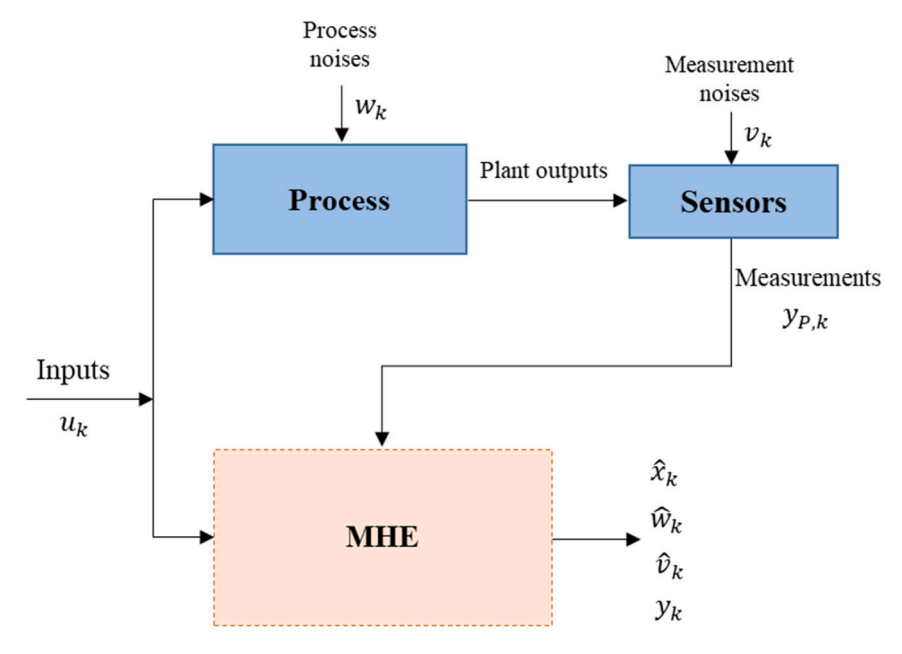


Fig. 2. Structure of the MHE estimation.

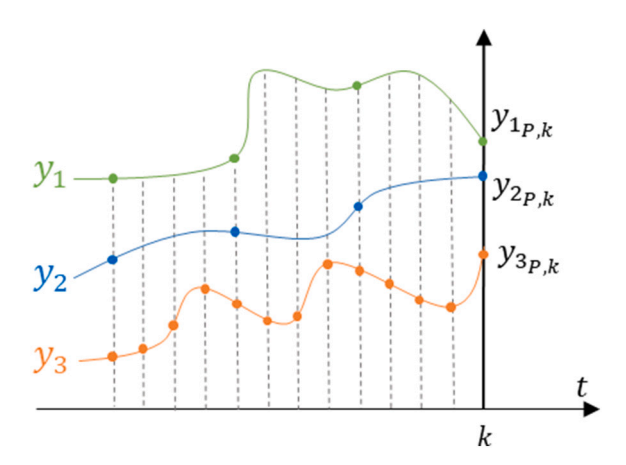


Fig. 3. Scenario considering a plant with multi-rate measurements.

the inoculum is summarized in Table 2.

Fig. 5 illustrates the daily variations in inflow and inlet wastewater concentrations for all components, as well as temperature and solar radiation. The inlet wastewater flow rate (Fig. 5 A) exhibits a trend consistent with the domestic wastewater flow data presented in [25]. The inlet concentration for each wastewater component is represented by the trend described in Fig. 5 B, in which the average wastewater concentration for each component is described in Table 1. The temperature and Photosynthetic Photon Flux Density (PPFD) values were evaluated in the context of summer conditions, as illustrated in Fig. 5 C and Fig. 5 D, respectively.

This study considers the availability of online pH, temperature, and dissolved oxygen measurements, with a sample period of 1.2 h. It is further assumed that daily measurements of dissolved Total Organic Carbon (TOC), dissolved ammonium $(N-NH_4^+)$, dissolved phosphate $(P-PO_4^{3-})$, and biomass concentration in the effluent are available for quality water monitoring. Additionally, the daily availability of measurements of biomass concentration in the HRAP and in the wastage flow rate is also assumed. The biomass concentration is quantified in terms of the Total Suspended Solids (TSS) concentration. It is hypothesized that the measurements of dissolved components are drawn from

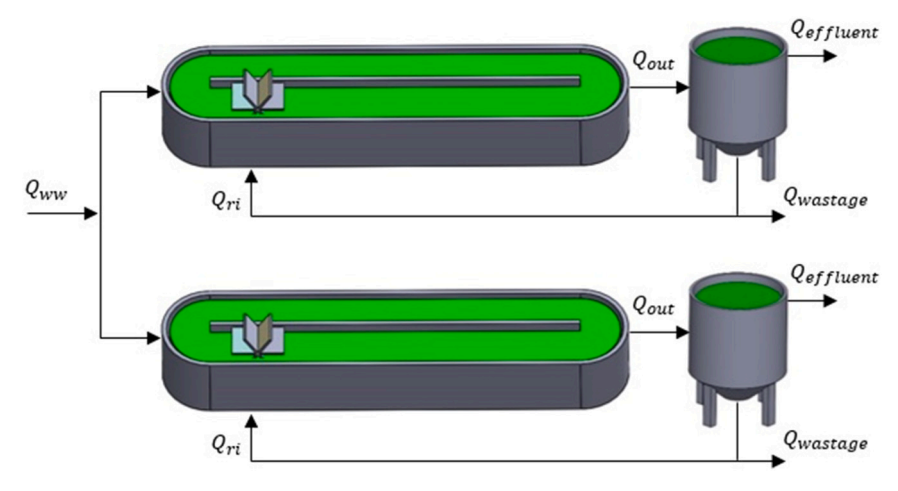


Fig. 4. Schematic of the hypothetical WWTP.

Table 1 Average inlet wastewater composition.

Component	Description	Concentration	Units
S _{NH4}	Ammonium nitrogen	45	${ m mgN-NH_4} \ { m L}^{-1}$
S_{NH3}	Ammonia nitrogen	0.15	${ m mgN-NH_3} \ { m L}^{-1}$
S_{NO3}	Nitrate nitrogen	0	${ m mgN-NO_3} \ { m L}^{-1}$
S_{NO2}	Nitrite nitrogen	0	$\begin{array}{c} \text{mgN-NO}_2 \\ \text{L}^{-1} \end{array}$
$S_{\rm CO2}$	Dissolved carbon dioxide	9.15	${ m mgC\text{-}CO_2} \ { m L}^{-1}$
S_{HCO3}	Bicarbonate	290	${ m mgC ext{-}HCO_3} \ { m L}^{-1}$
S_{CO3}	Carbonate	0.85	${ m mgC\text{-}CO_3} \ { m L}^{-1}$
$S_{\rm PO4}$	Phosphate phosphorus	8	${ m mgP\text{-}PO_4} \ { m L}^{-1}$
S_{O2}	Dissolved oxygen	0	$mgO_2 L^{-1}$
S_H	Hydrogen ions	0.000010	$mgH L^{-1}$
S _{OH}	Hydroxide ions	0.017008	mgH-OH L ⁻¹
S_S	Readily biodegradable soluble organic matter	100	${\rm mgCOD~L^{-1}}$
$S_{\rm I}$	Inert soluble organic matter	40	${\rm mgCOD~L^{-1}}$

Table 2
Inoculum composition.

Component	Description	Value	Units
X_{ALG}	Microalgae biomass	3550	${\begin{subarray}{c} { m mgCOD} \\ { m L}^{-1} \end{subarray}}$
X_{H}	Heterotrophic bacteria	592.85	${\begin{subarray}{c} { m mgCOD} \\ { m L}^{-1} \end{subarray}}$
X_{AOB}	Ammonium oxidizing bacteria	3.55	${ m mgCOD} \ { m L}^{-1}$
X_{NOB}	Nitrite oxidizing bacteria	1.775	${\begin{subarray}{c} { m mgCOD} \\ { m L}^{-1} \end{subarray}}$
X_S	Slowly biodegradable particulate organic matter	2463.7	${\begin{subarray}{c} { m mgCOD} \\ { m L}^{-1} \end{subarray}}$
X_{I}	Inert particulate organic matter	493.45	$\substack{mgCOD\\ L^{-1}}$

the HRAP, and that the concentration of dissolved components in the effluent is equal to that of the HRAP. The specific measurements and their respective sampling frequencies are summarized in Table 3.

2.3. Plant model

In this study, a detailed plant model was employed to simulate the dynamics occurring in the HRAP system with biomass recirculation. This sophisticated model was employed "in lieu" of the actual plant, and the measured variables are indeed the outputs of the detailed model.

2.3.1. HRAP model

The present study used the model BIO_ALGAE 2 [27] (with minor modifications as referenced in [28]) to represent the biochemical reactions and processes occurring within the HRAP. The model has previously undergone validation in HRAPs and other photobioreactor configurations under a range of operational conditions [27–30]. The model BIO_ALGAE 2 employs the standard nomenclature of the International Water Association models and considers 19 components –six particulate and 13 dissolved– involved as variables in the physical, chemical and biokinetic processes. These components are described, along with their primary roles in the processes and their interactions with other components, in [29]. The model BIO_ALGAE 2 encompasses processes related to microalgae and bacteria activity, light attenuation, photorespiration, temperature and pH dependence, and the transfer of gases from the algal-bacterial broth to the atmosphere. Details of the

process rates of the model, factors equations, and parameters used to represent the processes occurring in the HRAP are provided in Supplementary Material S1. The model's stoichiometric and kinetic parameters have been demonstrated to be valid for a broad spectrum of microalgae and bacteria employed in wastewater treatment applications [27,29–31]. To simulate the processes occurring in the HRAP, 22 state variables were utilized, including 19 state variables corresponding to model components and 3 state variables corresponding to the photosynthesis model.

In the BIO_ALGAE model, the compositions of the particulate components are expressed in terms of Chemical Oxygen Demand (COD). Therefore, it is necessary to perform the transformation from mgCOD/L to mgTSS/L to make a comparison with the measured data considered in the model. The COD/TSS ratios (Eqs. (8)–(9)) to perform this conversion were:

$$1 gVSS = 1.42 gCOD ag{8}$$

$$1 gTSS = 0.85 gVSS \tag{9}$$

Eqs. (10)–(11) related state model variables and measured variables.

$$TSS \left[mgSSTL^{-1} \right] = X_{ALG} + X_H + X_{AOB} + X_{NOB} + X_I + X_S$$
 (10)

$$TOC = i_{C.SS}S_s + i_{C.SI}S_I \tag{11}$$

where the names of the states X_i are defined in Table 2; $i_{C,SS}$ and $i_{C,SI}$ are the fraction of carbon in the readily biodegradable soluble organic matter (S_s) and in the inert soluble organic matter (S_I) , respectively, which corresponded to:

$$i_{C.SS} = 0.318 gC gCOD^{-1}$$

$$i_{C.SI} = 0.327gC gCOD^{-1}$$

2.3.2. Settler model

The settler was described using the mass-balance expressions of the Takács model [32]. The Takács model is a multi-layer dynamic model typically used for the clarification and thickening processes. In this work, a 10-layer settler was considered (this implies that 10 states were used to settler modeling). A comprehensive description of the settler model used in this work can be found in Supplementary Material S2.

2.4. Reduced model for state estimation

To create a more realistic framework for the application of the MHE technique, the detailed model previously referenced was utilized to simulate the "real plant," while a reduced model was employed for estimation with MHE. Given that this research was conducted within a simulation framework, the utilization of a reduced model in the estimation process enables the consideration of potential model uncertainties that invariably arise in practical applications. Furthermore, employing a lower-complexity model for estimation facilitates the reduction of estimation time, a critical factor in addressing nonlinear optimization problems.

The estimation developed in the present research is intended for further use in monitoring and controlling the quality of effluent water in a WWTP with microalgae and bacteria using the MPC strategy. The utilization of the state estimator in the context of effluent water quality monitoring can serve as a valuable instrument for enhancing the operational efficiency of the plant. By offering pertinent real-time information regarding the process's status, the state estimator can reduce the necessity for conducting analytical measurements, thereby facilitating more efficient management of the process. Similarly, the implementation of all real-time control and optimization strategies demands the knowledge of the actual state of the process.

The implementation of a control strategy within the WWTP should

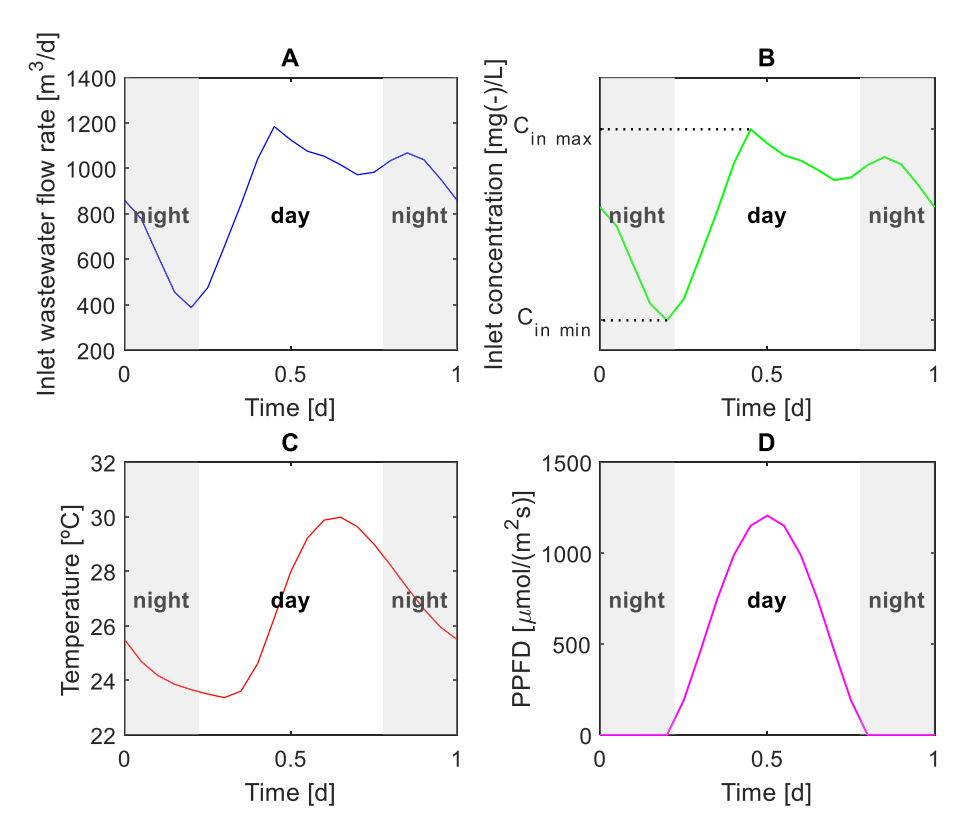


Fig. 5. Daily variation profiles of the inlet wastewater flow rate (A), inlet concentration (B), temperature (C), and photosynthetic photon flux density (D).

Table 3 Measured variables in the plant.

Measured variable [units]	Description	Type of measurement	Sampling frequency [samples/day]
S _{O2} [mgO ₂ / L]	Dissolved oxygen	Online	20
pH	pH in the HRAP	Online	20
T [°C]	Temperature in the HRAP	Online	20
TOC [mgC/ L]	Total organic carbon	Analytics	1
S _{NH4} [mgN- NH ₄ /L]	Dissolved ammonium	Analytics	1
S _{PO4} [mgP- PO ₄ /L]	Dissolved phosphate	Analytics	1
TSS _{HRAP} [mgTSS/L]	Total suspended solids concentration in the HRAP	Analytics	1
TSS _{effluent} [mgTSS/L]	Total suspended solids concentration in the effluent flow	Analytics	1
TSS _{wastage} [mgTSS/L]	Total suspended solids concentration in the wastage flow	Analytics	1

ensure compliance with the prevailing legislation (Directive 1/271/CEE for EU states). This directive establishes minimum requirements for the collection, treatment, and discharge of urban wastewater and wastewater from specific industrial sectors within the European Union. According to the directive, the evaluation of the quality of the treated wastewater discharged from urban WWTPs is to be based on the concentration of COD, TSS, total nitrogen, and total phosphorus in the effluent water. Therefore, components not directly associated with these variables are not necessarily subject to estimation by the MHE. Subsequently, the reduced model encompasses the estimation of the following variables:

- Biomass concentration (in the effluent flow, within the HRAP, and in the wastage flow). It is imperative to precisely monitor the TSS concentration in the effluent, as this is a critical factor in ensuring the desired quality of the water. Concurrently, the attainment of optimal biomass values within the HRAP is imperative to ensure sufficient wastewater treatment. The TSS concentration in the wastage flow is also estimated because in a system with recirculation, this value affects the TSS concentration in the HRAP. The biomass concentration is contingent upon the particulate components of the model, as delineated in Eq. (10). Of the biomass components, the concentration of nitrifying bacteria (X_{AOB} and X_{NOB}) was not incorporated into the reduced model. This was due to the fact that nitrifying bacteria, despite their acknowledged role in wastewater treatment, exhibited considerably lower concentrations compared to the other particulate components present in the HRAP.
- The ammonium concentration. Due to the main role of the ammonium over the microalgae growth and its influence in the total nitrogen concentration that should be guaranteed in the effluent wastewater. In the context of this particular study, the concentrations of nitrites and nitrates are significantly lower in comparison with other nitrogen species, such as ammonium. Consequently, the concentration of these variables was not considered in the reduced model. The legislation establishing limits for components concentrations stipulated values for total nitrogen, rather than for nitrites and nitrates.
- The phosphate concentration. Due to their influence over microalgae and bacteria growth. Additionally, the monitoring of phosphate concentrations is crucial for the overall assessment of total phosphorus in effluent wastewater.
- The dissolved oxygen concentration is a critical factor in achieving a
 comprehensive understanding of the primary processes within the
 HRAP. The availability of reliable online S_{O2} measurements, as well
 as the relation of the dissolved oxygen with the main process variables, allows for the design and implementation of state estimators
 based on dissolved oxygen measures.

 The TOC concentration, defined by Eq. (11) is directly related with the COD. Evaluating the COD is imperative to ensure efficient wastewater treatment.

The components of the inorganic carbon ($S_{\rm CO2}$, $S_{\rm HCO3}$, and $S_{\rm CO3}$) are not estimated by the reduced model because the focus of this study is on estimating those components regulated by the legislation that should be analyzed prior to the discharge. Consequently, the concentration of inorganic carbon is not regarded as a limiting factor in the discharge of effluent water.

In order to simplify the reduced model (and consequently improve the estimation time of the MHE), the concentration of $S_{\rm H}$ and $S_{\rm OH}$ was not calculated. In the reduced model, the pH of the culture medium is regarded as a known measured input.

Furthermore, the objective of minimizing the estimation time was pursued by calculating the factors of the photosynthesis model directly using the relations described in Table S3.2 of the Supplementary Material S3, as opposed to the system of differential equations utilized in the model of the plant (Table S1.2 of the Supplementary Material S1).

Summarizing, the reduced model of the HRAP included 10 state variables, as it was not necessary to estimate all components of the system for operation. A comprehensive summary of the state variables considered in both the real plant and MHE model is provided in Table 4.

The HRAP plant model encompasses 25 processes, including those related to the activity of autotrophic bacteria and the anoxic activity of heterotrophic bacteria. Conversely, the reduced model encompasses 10 processes, which are delineated in Table S3.1 of the Supplementary Material S3. A synopsis of the processes encompassed in the plant and the reduced model is summarized in Table 5. An analysis of Table 4 and Table 5 reveals the substantial structural disparities between the plant and the reduced model for the HRAP, as evidenced by the number of

Table 4State variables considered in the plant and in the reduced model.

	State variables	
	Considered in the plant [units]	Estimated by the reduced model (Yes/No)/Additional comment
	piant (units)	(1es/No)/Additional comment
HRAP model	X _{ALG} [mgCOD/L]	Yes
	X_H [mgCOD/L]	Yes
	X _{AOB} [mgCOD/L]	No
	X _{NOB} [mgCOD/L]	No
	X_S [mgCOD/L]	Yes
	X_I [mgCOD/L]	Yes
	S_{NH4} [mgN-NH ₄ /L]	Yes
	S _{NH3} [mgN-NH ₃ /L]	Yes
	S _{NO3} [mgN-NO ₃ /L]	No
	S _{NO2} [mgN-NO ₂ /L]	No
	S_{PO4} [mgP-PO ₄ /L]	Yes
	S_{O2} [mgO ₂ /L]	Yes
	S _{CO2} [mgC-CO ₂ /L]	No
	S _{HCO3} [mgC-HCO ₃ / L]	No
	S _{CO3} [mgC-CO ₃ /L]	No
	S _H [mgH/L]	No/ pH was considered as a measured
	S _{OH} [mgH-OH/L]	input in the reduced model
	S _S [mgCOD/L]	Yes
	S _I [mgCOD/L]	Yes
Photosynthesis	X ₁	No/Calculated directly, instead as
model	X_2	state variables
	X ₃	
Settler model	TSS _{effluent}	Yes
	TSS ₂	Yes
	TSS ₃	Yes
	TSS ₄	Yes
	TSS ₅	Yes
	TSS ₆	Yes
	TSS ₇	Yes
	TSS ₈	Yes
	TSS ₉	Yes
	TSS _{wastage}	Yes

Table 5
Processes considered in the plant and the model.

	Process	Plant	Model
Microalgae processes	Growth on S _{NH4}	Considered	Considered
	Growth on S _{NO3}	Considered	Not
			Considered
	Endogenous respiration	Considered	Considered
	Decay	Considered	Considered
Heterotrophic bacteria	Aerobic growth on S _{NH4}	Considered	Considered
processes	Aerobic growth on S _{NO3}	Considered	Not
			Considered
	Anoxic growth on S _{NO2}	Considered	Not
	(denitrification on S_{NO2})		Considered
	Anoxic growth on S _{NO3}	Considered	Not
	(denitrification on S_{NO3})		Considered
	Aerobic endogenous	Considered	Considered
	respiration		
	Anoxic endogenous	Considered	Not
	respiration		Considered
	Decay	Considered	Considered
Autotrophic bacteria	Growth of X _{AOB}	Considered	Not
processes			Considered
	Growth of X _{NOB}	Considered	Not
			Considered
	Endogenous respiration	Considered	Not
	of X _{AOB}		Considered
	Endogenous respiration	Considered	Not
	of X _{NOB}		Considered
	Decay of X _{AOB}	Considered	Not
			Considered
	Decay of X _{NOB}	Considered	Not
			Considered
Hydrolysis	Hydrolysis	Considered	Considered
Chemical equilibrium	Chemical equilibrium	Considered	Not
	$CO_2 \leftrightarrow HCO_3^-$		Considered
	Chemical equilibrium	Considered	Not
	$HCO_3^- \leftrightarrow CO_3^{2-}$		Considered
	Chemical equilibrium	Considered	Considered
	$NH_4^+ \leftrightarrow NH_3$		
	Chemical equilibrium	Considered	Not
	$H^+ \leftrightarrow OH^-$		Considered
Transfer of gases	S_{O2} transfer to the	Considered	Considered
	atmosphere		
	S_{CO2} transfer to the	Considered	Not
	atmosphere		Considered
	S_{NH3} transfer to the	Considered	Considered
	atmosphere		

states and equations involved. Additionally, disparities in the values of some parameters were considered in plant and model (Table 6). The values of the parameters in the plant were selected based on the values previously reported in the literature for microalgae-bacteria raceway reactors [29,31]. The settler model used for estimation, similarly with the one used for plant simulation, encompasses also 10 state variables.

The simulated differences between the plant and the reduced model starting from the initial inoculation time of the plant are illustrated in Fig. 6-Fig. 10 for a period of 60 days operating under the conditions illustrated in Fig. 5. The initial values of the states set in the plant and model simulation are described in the Supplementary Material S4. The differences in the concentration of particulate components in the HRAP are shown in Fig. 6. The biomass concentration into the raceway reactors, in the effluent flow, and in the wastage flow for the plant and the reduced model are illustrated in Fig. 7. The effect of daily variations over

Table 6Values of parameters in plant and model.

Parameter [units]	Description	Plant	Model
$\mu_{ALG} [d^{-1}]$	Maximum specific growth rate of microalgae	2.5	3.5
$\mu_{\mathrm{H}} \ [\mathrm{d}^{-1}]$	Maximum specific growth rate of heterotrophic bacteria	5.8	5.5
$K_{la, O2} [d^{-1}]$	Mass transfer coefficient for oxygen	10	9

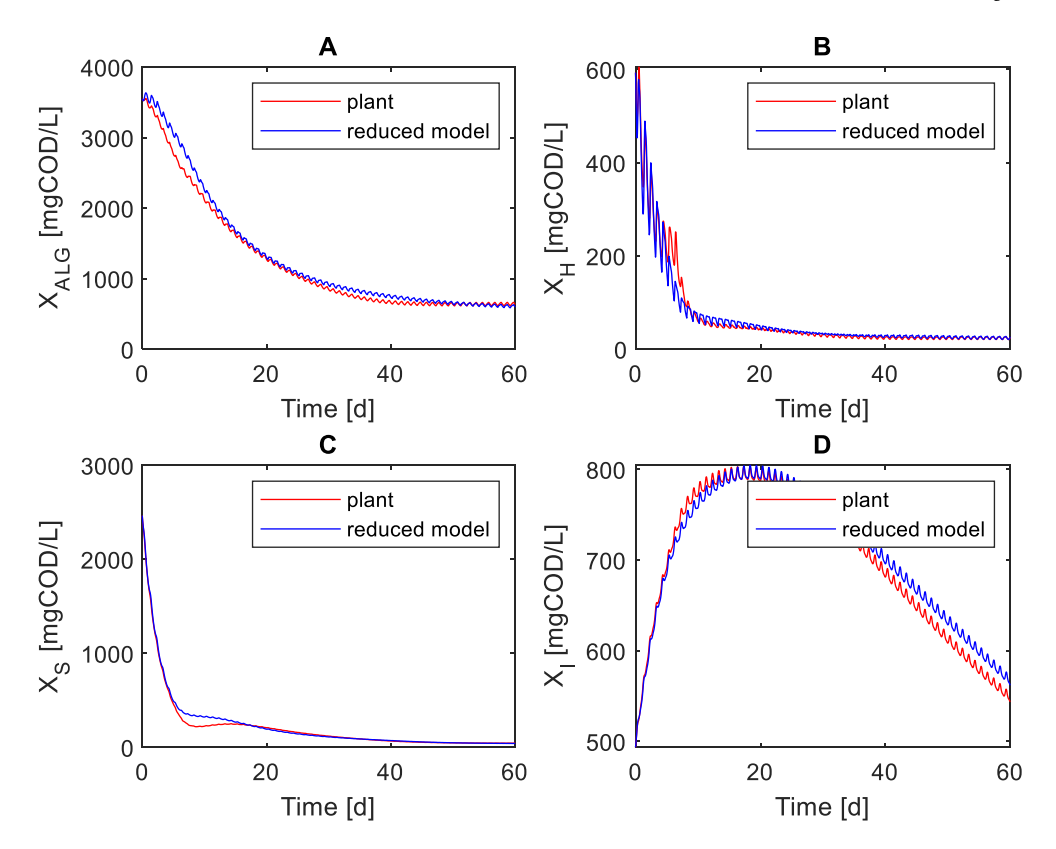


Fig. 6. Plant and reduced model differences in the biomass composition in the HRAP: microalgae biomass (A), heterotrophic bacteria (B), slowly biodegradable particulate organic matter (C), and inert particulate organic matter (D).

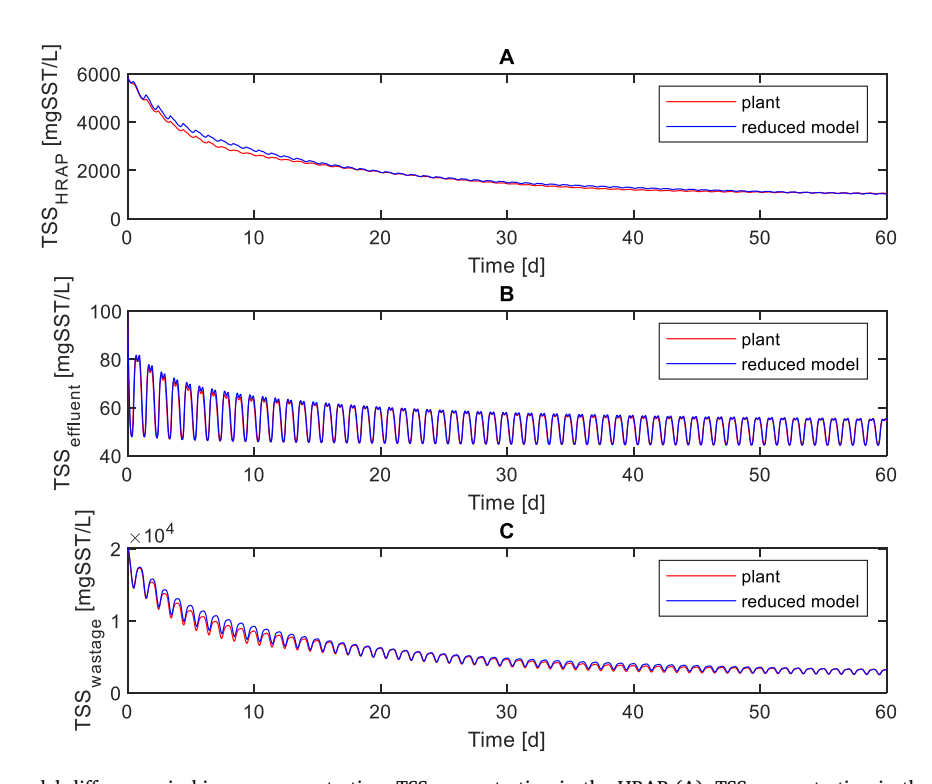


Fig. 7. Plant and reduced model differences in biomass concentration: TSS concentration in the HRAP (A), TSS concentration in the effluent flow (B), and TSS concentration in the wastage flow (C).

the biomass due to operational and environmental variables is visible in both the plant and model trend. The concentration of the dissolved components in the HRAP is illustrated in Fig. 8, where the ammonium

and phosphate assimilation by microalgae (Fig. 8A and B, respectively) was highly affected by day/night cycles, as well as the TOC assimilation by heterotrophic bacteria (Fig. 8C). Concomitantly, substantial

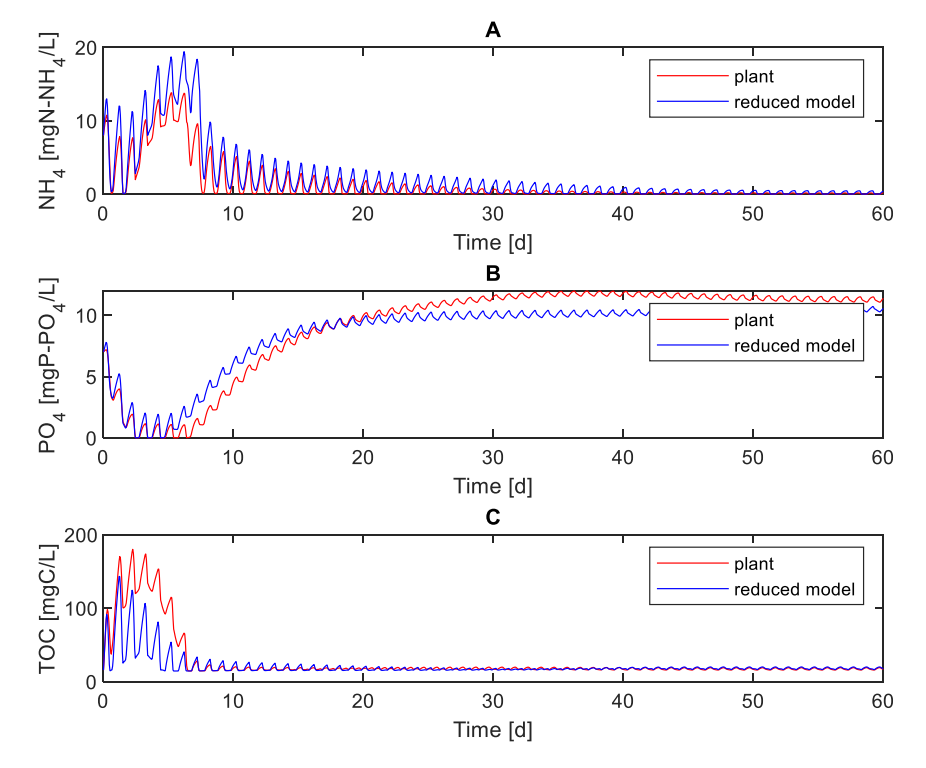


Fig. 8. Plant and reduced model differences in the dissolved ammonium concentration (A), the dissolved phosphate concentration (B), and the dissolved total organic carbon concentration (C) in the HRAP.

variations in the dissolved oxygen concentration within the HRAP, attributable to diurnal fluctuations in irradiation, are evident in both the plant and in the reduced model (Fig. 9). States of the photosynthesis model are represented in Fig. 10 for the plant and the reduced model. The analysis of Fig. 6-Fig. 10 reveals that the reduced model effectively replicates the trend of the primary variables involved in wastewater treatment. This finding validated its use as a prediction model in the MHE approach. Conversely, the discrepancies in the behavior of the reduced model in comparison to the plant depicted in Fig. 6 to Fig. 10 can be attributed to two primary factors: structural mismatches (summarized in Table 4 and Table 5) and parameter mismatches (detailed in Table 6).

2.5. Software and hardware

The MHE was coded using MATLAB® software [33], version 24.1, R2024a and the MPCTools [34]. MPCTools is a control and estimation tool for linear and nonlinear dynamic models, and it provides an oriented interface to CasADi for Octave and MATLAB®. The estimation problem was addressed by employing the Ipopt (Interior Point Optimizer) solver, which is an open-source software package for large-scale nonlinear optimization. The model used for estimation was discretized using the Runge-Kutta method. The MHE simulations were carried out with the following computer hardware specifications: an 13th Gen Intel® Core $^{\text{TM}}$ i9-13900K processor (3.0GHz), 128 GB RAM memory, and a 500 GB hard-disk drive.

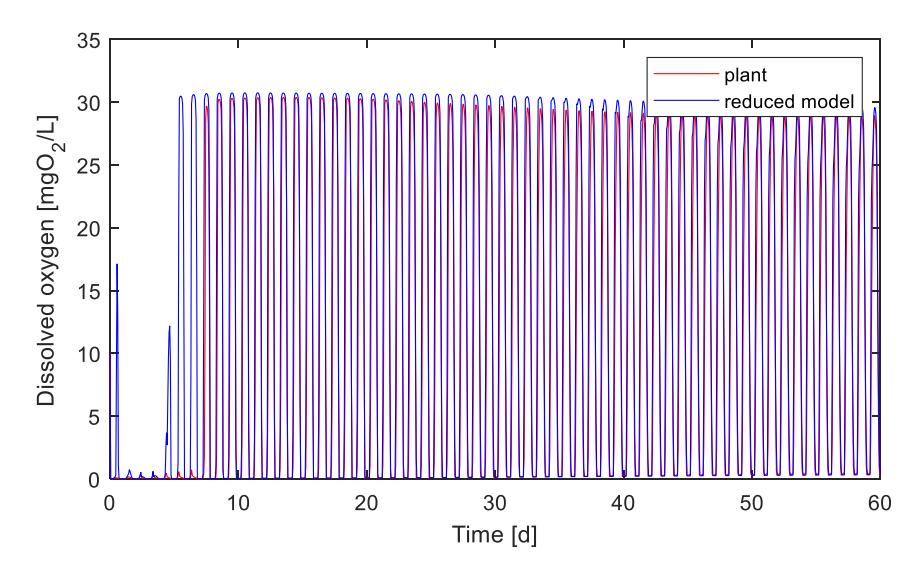


Fig. 9. Plant and reduced model differences in the dissolved oxygen concentration in the HRAP.

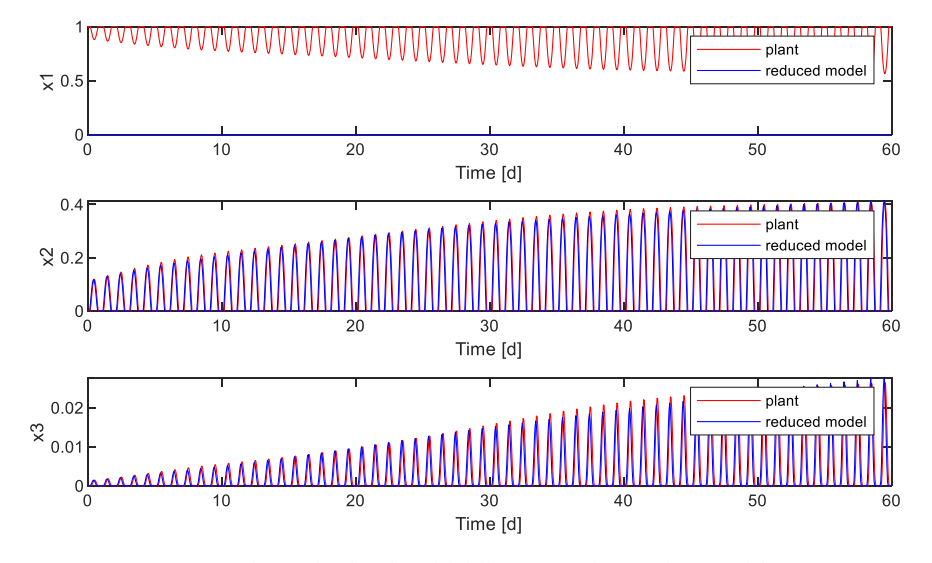


Fig. 10. Plant and reduced model differences in photosynthesis model.

3. Results and discussion

3.1. State estimation using MHE in microalgae-bacteria wastewater treatment plant

MHE was designed to furnish the values of the unmeasured states for prospective implementations of model predictive control algorithms and optimization strategies to enhance system performance. These unmeasured states offer critical information about the system, which is essential for the effective implementation of feedback control strategies. The application of MHE to microalgae-based wastewater treatment systems poses specific challenges, primarily due to i) the scarcity of online measurements, ii) the lack of perfect knowledge of the model structure, iii) uncertainties in the values of parameters and states, iv) the unavailability of direct methods to determine the fractions of particulate components in the biomass, v) the reliability of analytical measurements is highly dependent on human expertise, vi) the elapsed time from the moment the sample is taken to the moment the analytical procedure is completed.

In the hypothetical microalgae-based WWTP studied in this work,

multi-rate measurements are presented with the sampling frequency shown in Table 3. Online measurements of the high-rate dynamic variables (pH, temperature, and dissolved oxygen) could be available with a higher sampling time. However, the sampling time of 1.2 h was used considering the slow dynamics of these variables in a large treatment plant and to avoid excessive computational time in the optimization. The estimator takes into account the availability of irradiance, pH, temperature, and flow measurements. The schematic of the MHE applied to the case study is depicted in Fig. 11.

The structure of the state, output, and input vectors employed in the MHE formulation are described by Eqs. (12)–(14):

$$\mathbf{x} = \begin{bmatrix} X_{ALG} & X_{H} & X_{S} & X_{I} & S_{S} & S_{I} & S_{NH4} & S_{NH3} & S_{PO4} & S_{O2} & TSS_{effluent} \end{bmatrix}^{T}$$

$$TSS_{2} \quad TSS_{3} \quad TSS_{4} \quad TSS_{5} \quad TSS_{6} \quad TSS_{7} \quad TSS_{8} \quad TSS_{9} \quad TSS_{wastage} \end{bmatrix}^{T}$$

$$\mathbf{y}_{P} = \begin{bmatrix} TSS_{HRAP} & TOC_{HRAP} & S_{NH4} & S_{PO4} & S_{O2} & TSS_{effluent} & TSS_{wastage} \end{bmatrix}^{T}$$

$$(13)$$

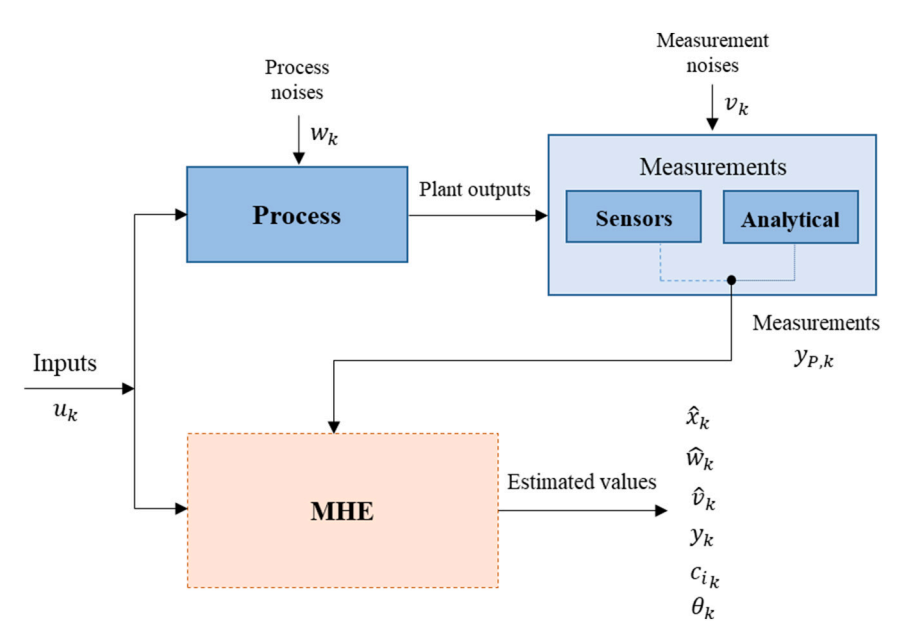


Fig. 11. Schematic of MHE for the microalgae-based WWTP.

$$\mathbf{u} = \begin{bmatrix} I & pH & T & Q_{ww} & Q_{ri} & Q_{wastage} \end{bmatrix}^T \tag{14}$$

The naming of the state variables to estimate (Eq. (12)) is detailed in Table 1 and Table 2 and Table S4.2 in Supplementary Material S4. The measurement vector, as developed by Eq. (13), encompasses the variables enumerated in Table 3. In the MHE formulation, the vector of known inputs, defined by Eq. (14), includes the values of irradiance (I), pH (pH), and temperature (T) of the culture media, as well as the values of inlet wastewater flow (Q_{ww}), recirculation flow (Q_{rl}), and wastage flow ($Q_{wastage}$).

The MHE is intended to estimate the state vector values at each sampling time (\mathbf{x}) , as well as the values of the unknown disturbances (\mathbf{w}) and measurement noises (v) that minimize the cost function defined in Eq. (1). In order to obtain useful information for system operation and control, the values of the input wastewater concentration c_i (Eq. (15)) and the values of relevant process parameters (vector θ , Eq. (16)) are also decision variables in the optimization problem. Estimated parameters are instrumental in characterizing the microbial dynamics in the process. In this sense, the maximum specific growth rates of microalgae (μ_{ALG}) and heterotrophic bacteria were estimated $(\mu_H),$ as well as the decay rate of microalgae ($k_{death,ALG}$) and heterotrophic bacteria ($k_{death,H}$). Concurrently, the estimation of the mass transfer coefficient of the dissolved oxygen was conducted ($K_{la,O2}$). In previous research works that employed the same model, a sensitivity analysis was conducted [28], thereby identifying these parameters as the most relevant parameters to adjust. Concurrently, these parameters were identified as the most influential parameters in other pertinent publications in the field [27,29].

$$c_i = [S_{S_{ww}} \quad S_{I_{ww}} \quad S_{NH4_{ww}} \quad S_{NH3_{ww}} \quad S_{PO4_{ww}}]^T$$
 (15)

$$\theta = \begin{bmatrix} \mu_{ALG} & k_{death,ALG} & \mu_{H} & k_{death,H} & K_{la,O2} \end{bmatrix}^{T}$$
(16)

Given the availability of multi-rate measurements, the execution time of the MHE is determined by the fastest measurements (dissolved oxygen measurements). It is assumed that analytical measurements are available daily at 0 a.m., implying that a full vector of output measurements is only available on a daily basis. Conversely, at each sampling time $(1.2\,\mathrm{h})$, a new dissolved oxygen measurement is available. An overview of the availability of measurements is given in Table 3. To address the challenge posed by multi-rate measurements in the context of MHE, two decisions were made:

- The consideration of a past horizon, encompassing at least a full vector of output measurements (the estimation past horizon should be a minimum of 1 day).
- The cost function incorporates only the available measurements at each sampling time.

3.1.1. MHE tuning

In order to formulate MHE, it is necessary to provide the values of the weight matrices of the cost function, as defined by Eq. (1). It is imperative to note that Q_x , Q_w , and Q_y are positive definite matrices, with weighting and normalization factors. The weight Q_x serves to penalize the error in the estimation at the beginning of the horizon, thereby indicating the reliability of the estimation. Given the imprecise nature of the initial guesses for the states, the diagonal elements of $\mathbf{Q}_{\mathbf{r}}$ are set to a value of 0.5. Table S5.1 and Table S5.2 of the Supplementary material S5 present the values of the diagonal elements of \boldsymbol{Q}_{w} and $\boldsymbol{Q}_{y},$ respectively. The tuning values of Q_w and Q_y were selected based on the standard deviation of the variables in order to normalize the different terms of the cost function. In the WWTP, considerable scale differences in the measured output variables, as well as in the estimated states, necessitated the normalization of these values. This procedure was implemented with the objective of ensuring that each output was accorded equal importance, as well as to guarantee the same importance in the modeling error for each estimated state. The weight values were selected

to allocate greater importance to the discrepancies between the model and the measurements, indicating that the reliability of the measurements surpasses that of the model. The constraints on the variables involved in the optimization problem are summarized in Table S5.3 through Table S5.6 of the Supplementary Material S5.

3.2. MHE simulation results

The results of the MHE execution are presented considering the system operation under a periodic regime. The parameters utilized in the MHE simulation are enumerated in Table 7. The estimation horizon of two days is regarded as sufficient in terms of data availability to support the calculation of an accurate estimation. In the context of the MHE application, it is imperative to align the sampling period with the dynamics of the variables to be estimated. The application under consideration in this research involves the estimation of variables related to water quality. The variables in question exhibit slow dynamics, thereby rendering lower sampling times unnecessary. Despite the fact that commercial sensors for dissolved oxygen measurement provide data with considerably lower sampling times than those employed in the present research, the sampling time used in this paper was selected considering that large estimation times are generally needed for nonlinear estimation with constraints. Moreover, in order to consider the possible applications of the MPC control strategy in this process, it is essential that the sampling time be adequately long to encompass both the estimation time and the time required for executing the nonlinear constrained MPC controller.

Simulations were executed under the environmental conditions illustrated in Fig. 5. Additionally, to simulate possible measurement errors in sensors and analytical procedures, a measurement noise was introduced. This noise was generated using a MATLAB® function which returns a random scalar drawn from the standard normal distribution. For each output, the media of the noise value introduced corresponds to 5 % of the average output value. The simulation results for the MHE application during 3 days (corresponding with 60 samples) are presented in Fig. 12 to Fig. 16, using initial information of past data corresponding to two previous days. In each sample, the MHE estimation was provided with an average value of 17.97 s (the higher estimation time being 37.49 s), which means that MHE can be used as the first step of advanced control or process dynamic optimization.

The estimated values (blue line) for the dissolved oxygen concentration in the HRAP are illustrated in Fig. 12. The red line in the graph represents the actual values of the dissolved oxygen concentration, which include the noise in the measurements. As this study was conducted within a simulation framework, real-time plant values are available for continuous representation, with the purpose of illustrating the estimator fit. In real-world scenarios, the measured values are only available at discrete time intervals, which are represented by crosses in the data. Error bars (purple bars) are included to illustrate the limits of uncertainty that were assumed in the measurements. The results demonstrate the accuracy of the prediction provided by the MHE, as well as estimator robustness, even considering noisy measurements.

The estimated values for the biomass concentration in the HRAP, the biomass concentration in the effluent, and the biomass concentration in the wastage stream are illustrated in Fig. 13. As demonstrated in Fig. 13, the MHE effectively estimates the biomass concentration values for the entire simulation time by leveraging historical output values and dissolved oxygen measurements at each sampling time. The error bars represent the uncertainties in the measured values of the biomass. In

Table 7 MHE simulation parameters.

Parameter	Description	Value
n_e	Estimation horizon	2 d (40 samples)
Delta	Sampling time	0.05 d

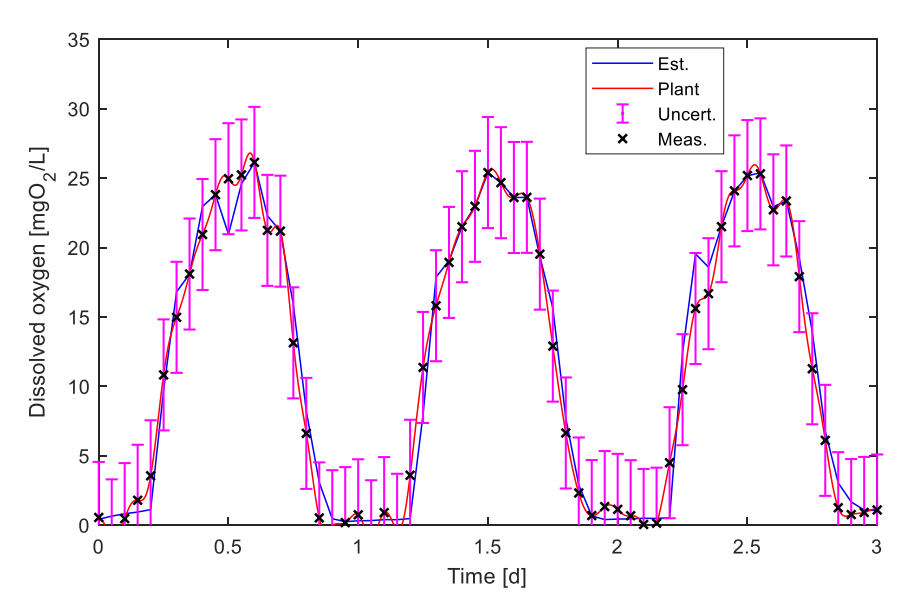


Fig. 12. Measured and estimated values of the dissolved oxygen in the HRAP.

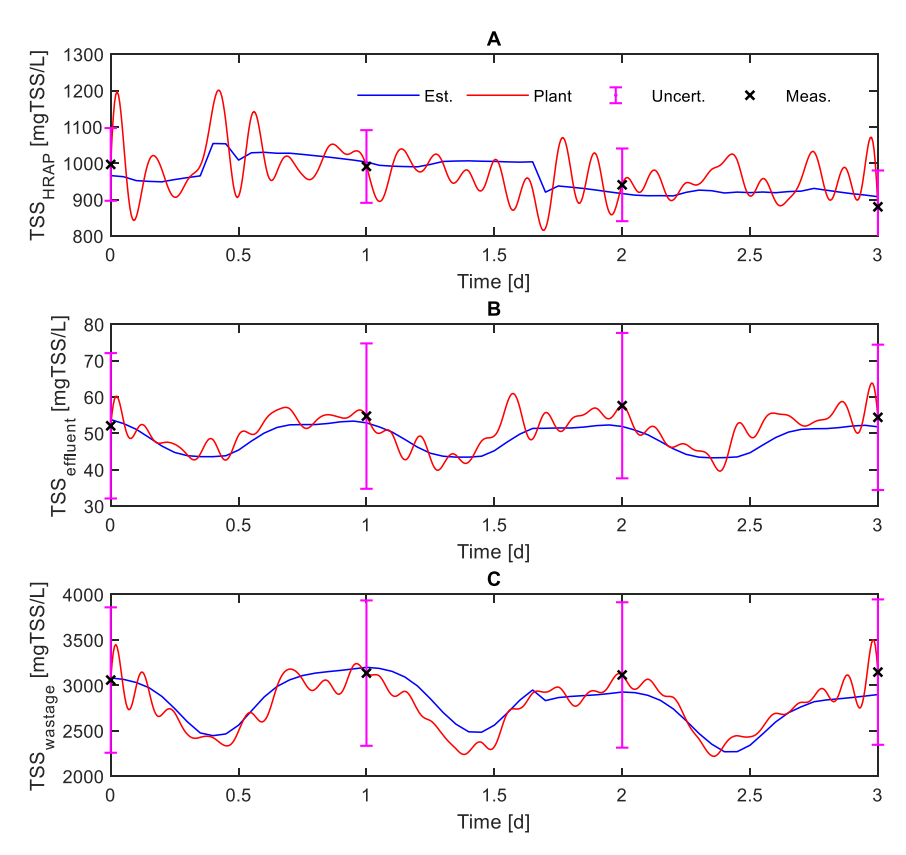


Fig. 13. Measured and estimated values of the biomass concentration in the HRAP (A), in the effluent (B), and in the wastage stream (C).

such cases, where analytical procedures are employed to ascertain biomass values, low biomass values are deemed to be more susceptible to measurement uncertainties. The online estimation of biomass concentration is imperative for ensuring the optimal operation of photobioreactors taking early actions in response to the values of the estimated variables, without waiting for the lab analysis to arrive. Optimal biomass values in the HRAP are necessary to ensure the adequate wastewater depuration, and high biomass concentrations within the reactor affect the penetration of solar radiation into the culture, which in turn affects the growth of microalgae. In addition, the

online monitoring of TSS concentration in the effluent is of a paramount importance in order to guarantee the desired water quality. Conversely, in scenarios where the primary objective is the harvesting of biomass for the production of diverse bioproducts, it is essential to optimize biomass yield to ensure maximum economic profitability.

The MHE has the capacity to predict the values of the various components of biomass (Fig. 14). Conventionally, the assessment of these values does not employ direct or standardized methodologies. Indeed, a salient benefit of the application of state estimators in such processes is that they enable the estimation of the concentrations of different

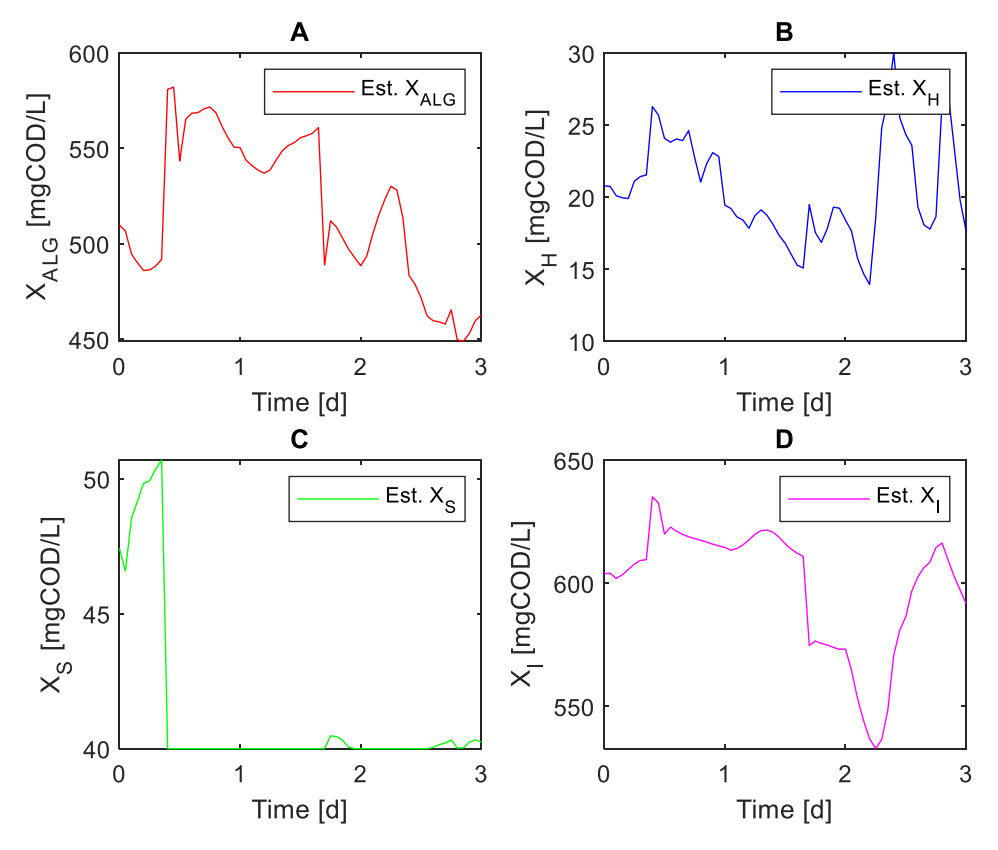


Fig. 14. Estimated values of the biomass components: microalgae biomass concentration (A), heterotrophic bacteria concentration (B), slowly biodegradable particulate organic matter (C), and inert particulate organic matter (D).

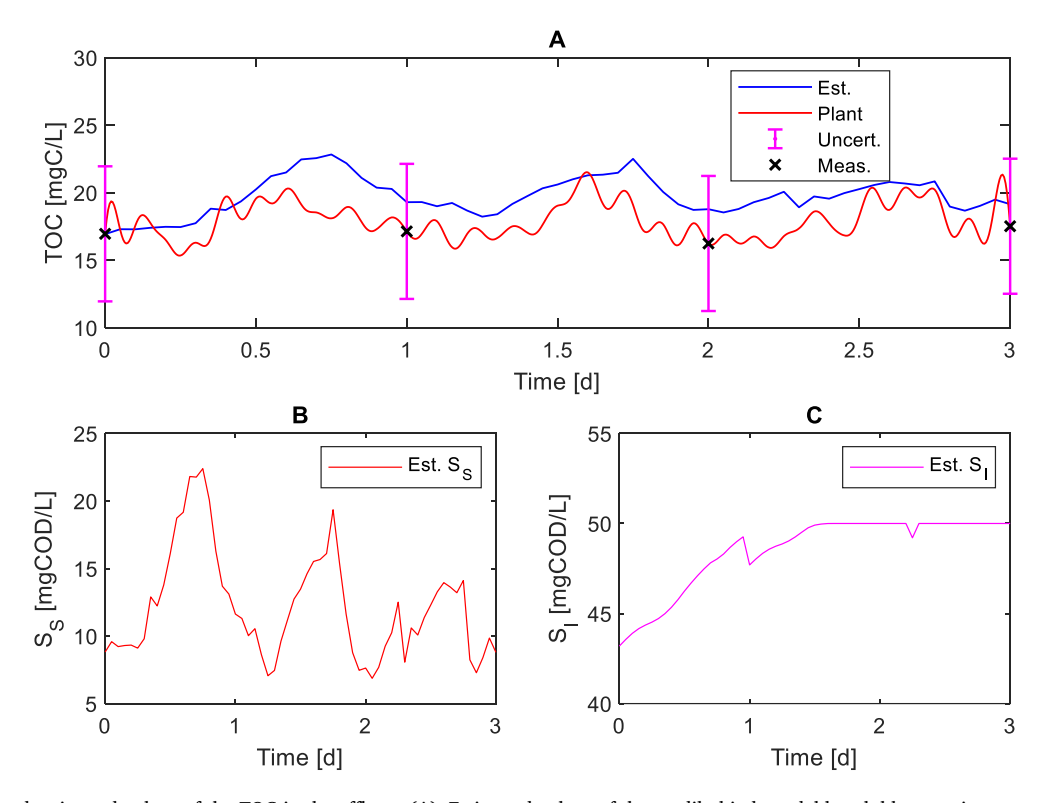


Fig. 15. Measured and estimated values of the TOC in the effluent (A). Estimated values of the readily biodegradable soluble organic matter (B) and inert soluble organic matter (C).

biomass components without the necessity of employing complex analytical methods.

The measured and estimated values of the TOC in the effluent are presented in Fig. 15 A. The online monitoring of the TOC concentration is imperative for the evaluation of effluent water quality. Fig. 15 B and Fig. 15 C illustrate the estimated values of readily biodegradable soluble organic matter and inert soluble organic matter, respectively, as TOC. The quality of effluent water is also contingent upon the concentrations of dissolved ammonium and dissolved phosphate. The measured and estimated values of dissolved ammonium and dissolved phosphate concentration are illustrated in Fig. 16 A and Fig. 16 B, respectively. As demonstrated in Fig. 16 A, the estimate of the ammonium concentration in the effluent exhibits a slight overestimation relative to the actual value. This phenomenon can be attributed to the observation that the proliferation of microalgae and heterotrophic bacteria (the two predominant microorganisms groups in the HRAP) is exclusively associated with the utilization of ammonium. This association disregards the microalgae growth on S_{NO3}, as well as the heterotrophic bacteria aerobic growth on nitrate and the heterotrophic bacteria anoxic growth on nitrite and nitrate (as summarized in Table 5). This finding suggests that the reduced model attributes the observed growth exclusively to nitrogen species in the form of S_{NH4}, which may lead to an overestimation of this component in the HRAP. In a similar fashion, the phosphate estimation (Fig. 16 B) exhibits a slight increase compared to the actual value of S_{PO4} concentration. This discrepancy can be attributed to the reduced model incorporating a smaller number of nutrients utilized by microalgae and bacteria for its growth, resulting in an overestimation of these components within the reduced model. Nevertheless, these discrepancies between the actual and estimated values are acceptable given the variation range of these components, as well as the potential inaccuracies in the analytical procedures employed to obtain the actual values of these variables. The validity of this assertion is supported by the results presented in Fig. 15 and Fig. 16. These figures demonstrate that the estimated values fall within the uncertainty limits that have been established in the measurement of these variables.

The MHE approach assessed in this study effectively estimated the concentrations of particulate and soluble components in the WWTP, even when a limited number of samples are available. These results suggest that further enhancement of the application of control and

optimization strategies in wastewater treatment plants is possible.

Despite the existence of analytical measurements on a daily basis, the employment of a state estimator offers insights into the progression of wastewater components throughout the entirety of the experimental period, a situation that has been previously observed in simulation results. State estimators serve as instrumental tools for the analysis of water quality over the course of a day. Leveraging this analysis, control actions can be implemented in a targeted and informed manner. As illustrated in Fig. 16 A, which depicts the time course of dissolved ammonium concentration, there is a demonstrable variation in the dynamics of dissolved ammonium over the course of a day. Specifically, higher values of ammonium are observed during nocturnal hours, which can be attributed to the assimilation of dissolved ammonium by microalgae during daylight hours. Given that the samples were hypothesized to be drawn during the night, these values are representative of a particular moment in the process dynamics evolution, which underscores the importance of continuous state estimation.

Parameter estimation is paramount for characterizing the kinetics of the key processes and chemical reactions, as well as the operational conditions in the HRAP. The results of parameter estimation for the parameters described by Eq. (16) are provided in Fig. 17. As demonstrated in Fig. 17, the estimated parameters exhibited a high degree of proximity to the "real values" of the parameters assumed in the plant. As demonstrated in Fig. 12 - Fig. 16, the simulation results substantiate the validity of the selected parameter values for predicting the process's state evolution. In order to ensure the effective implementation of model-based control strategies within the WWTP, it is imperative to establish precise parameter estimations.

In order to evaluate the robustness of the estimator under different operational conditions, variations in the incident light were considered during the third day of the estimation process. As illustrated in Fig. 18, the radiation profile under consideration consists of two days with identical radiation conditions to those previously illustrated in Fig. 5 D, and a third day characterized by substantial cloud cover. The estimation results for this condition are illustrated in Fig. 19 - Fig. 21. The dissolved oxygen concentration in the HRAP under fluctuating solar radiation is depicted in Fig. 19, where it is demonstrated that the available solar radiation during the third day of operation affects the maximum values of dissolved oxygen concentration in the photobioreactor, owing to a

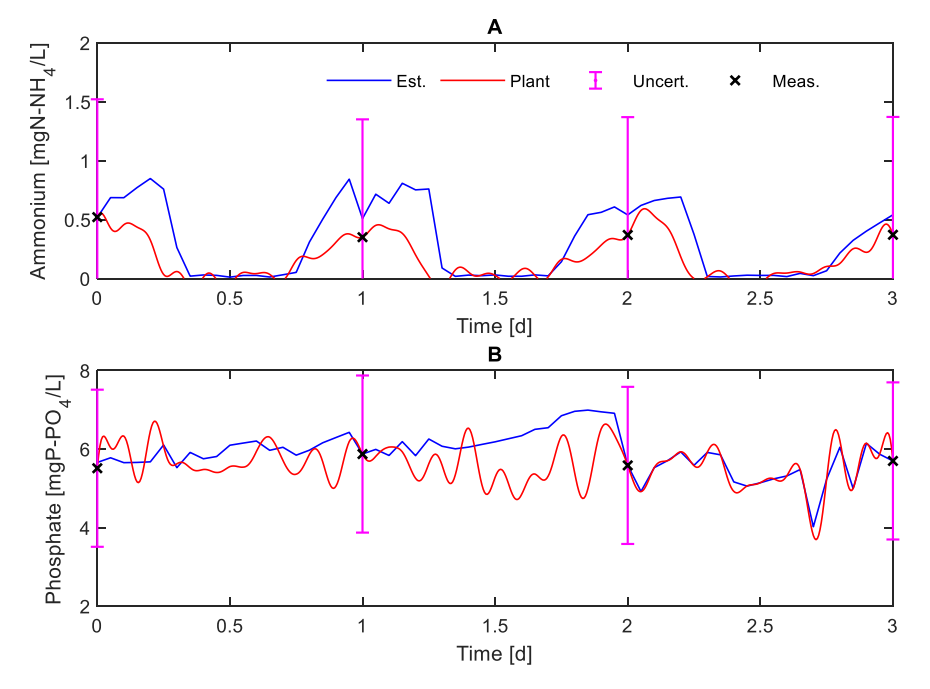


Fig. 16. Measured and estimated values of the dissolved ammonium concentration (A) and dissolved phosphate concentration (B).

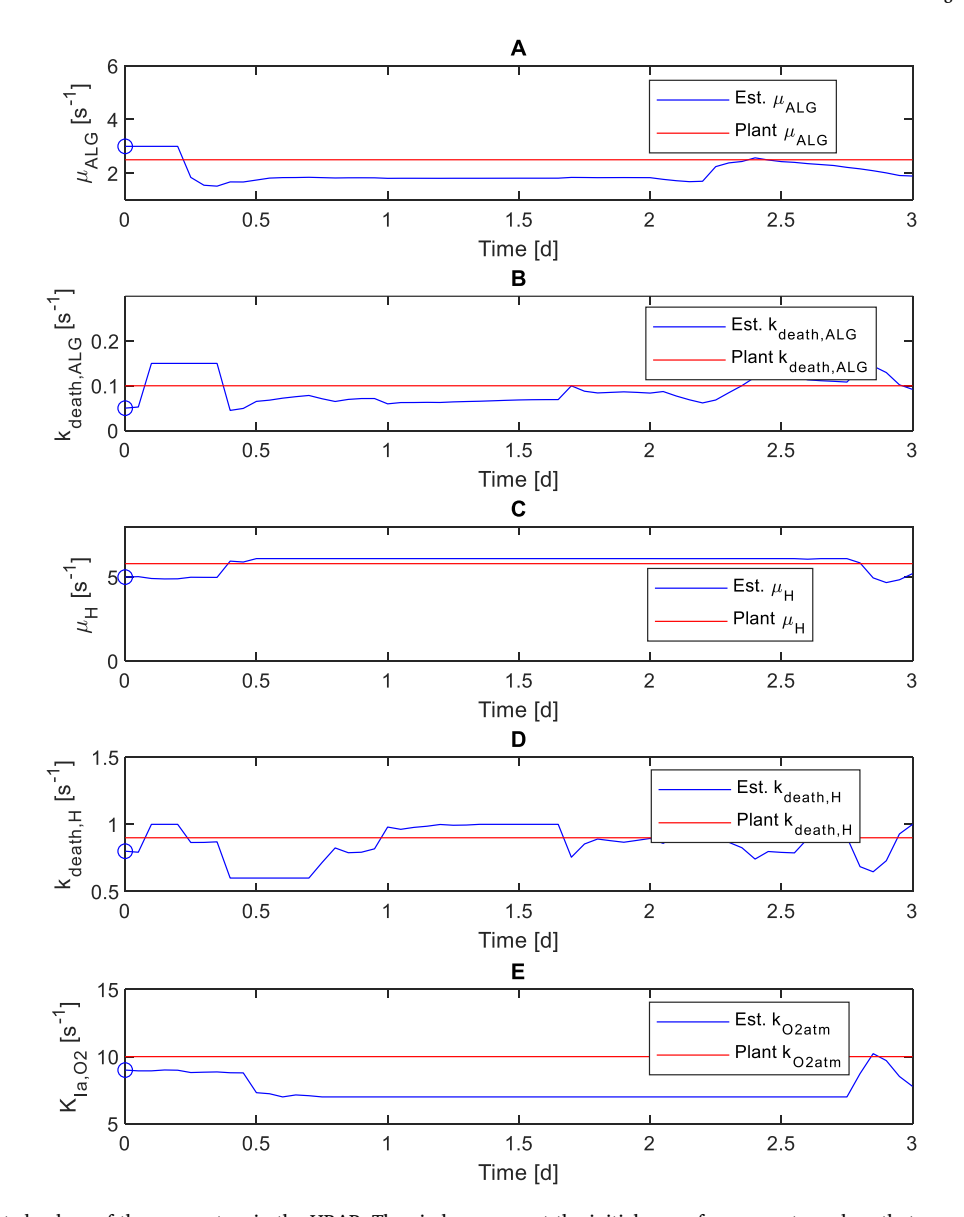


Fig. 17. Real and estimated values of the parameters in the HRAP. The circles represent the initial guess for parameter values that were utilized in the optimization problem.

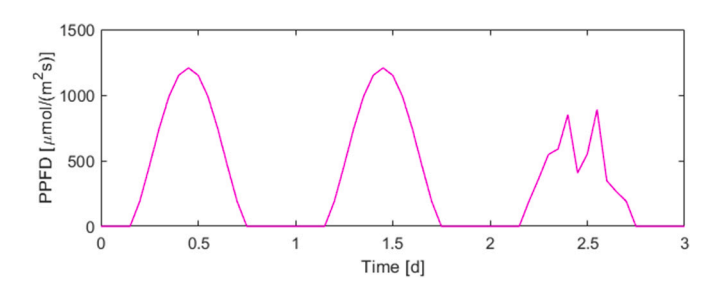


Fig. 18. Profile of the photosynthetic photon flux density considered over the course of three days of operation.

decline in microalgae activity. The effectiveness of the estimator in reproducing the trend in the dissolved oxygen concentration serves as a testament to its reliability in a variety of environmental conditions and in the presence of noisy measurements. This reliability is indicative of the robustness of the estimator.

Fig. 20 illustrates the measured and estimated values of biomass concentration under fluctuating solar radiation and also demonstrates

the robust behavior of the estimator, effectively replicating the measured values of biomass concentration in the HRAP (Fig. 20~A), the effluent flow (Fig. 20~B), and the wastage flow (Fig. 20~C).

The performance of the estimator in predicting the concentration of dissolved components in the HRAP under fluctuating solar radiation is illustrated in Fig. 21. Predicted values of the dissolved total organic carbon concentration (Fig. 21 A), ammonium concentration (Fig. 21 B), and phosphate concentration (Fig. 21 C) demonstrate slight overestimation, as previously evidenced in simulation results. Nevertheless, the discrepancies observed in these estimations fall within the permissible uncertainty range (as indicated by the error bars), even in the presence of significant environmental variations and unreliable measurements.

The simulation results demonstrate the efficacy of the MHE approach in online estimation of the most relevant variables of a wastewater treatment process, even in the presence of noisy measurements, model inaccuracies, varying environmental conditions, and multi-rate measurements. The MHE has the capacity to provide online estimation for measured variables and for variables that cannot be measured directly. The findings, in conjunction with the reduced estimation times

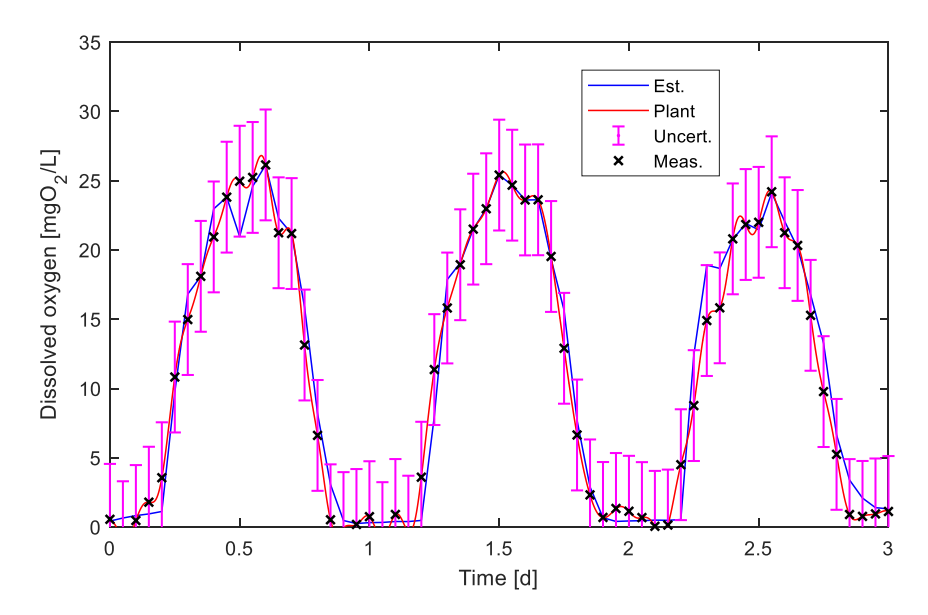


Fig. 19. Measured and estimated values of the dissolved oxygen in the HRAP under fluctuating solar radiation.

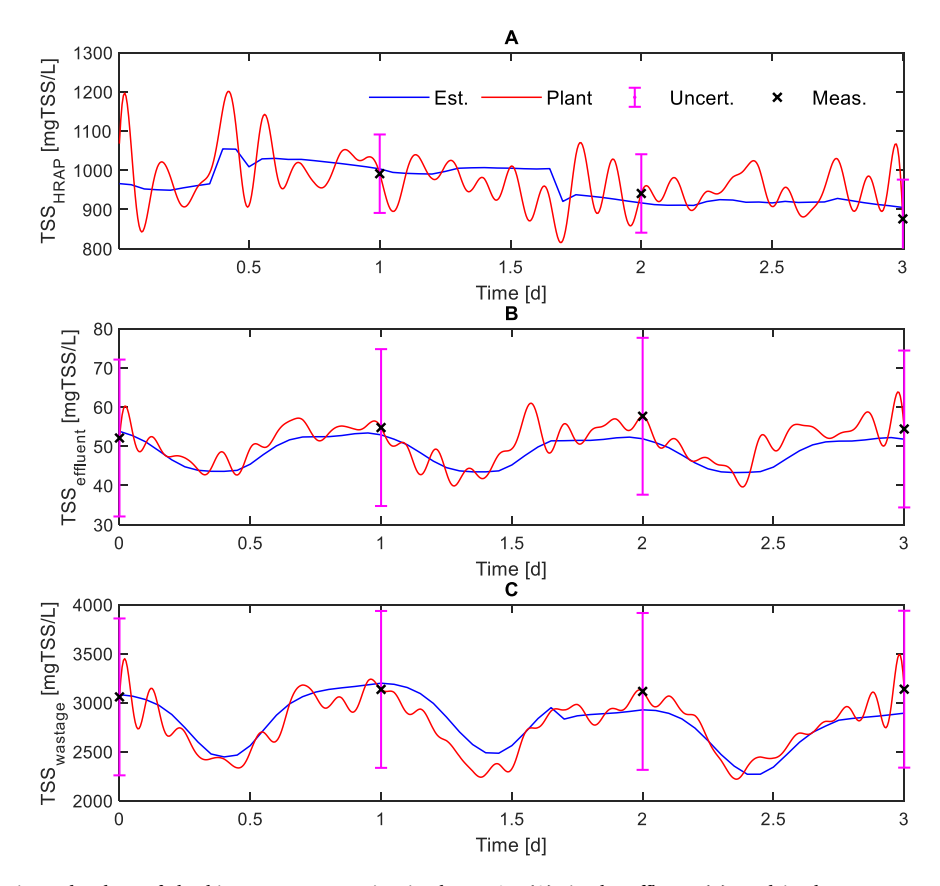


Fig. 20. Measured and estimated values of the biomass concentration in the HRAP (A), in the effluent (B), and in the wastage stream (C) under fluctuating solar radiation.

observed, underscore the promise of state estimation leveraging the MHE technique in conjunction with control and optimization strategies within wastewater treatment facilities, particularly in the context of low dynamics that characterize wastewater treatment processes.

4. Conclusions

The present study proposes the utilization of MHE technique for a

microalgae-based wastewater treatment process, with a focus on the estimation of multiple states and parameters concurrently to evaluate the effluent water quality. This work used an estimation model with multiple states and parameters, incorporating a substantial structural mismatch between the model used for estimation and the actual plant. Multi-rate measurements obtained from online measurements and analytical procedures were used to enhance the performance of the estimator. The simulation results confirmed the efficacy and robustness

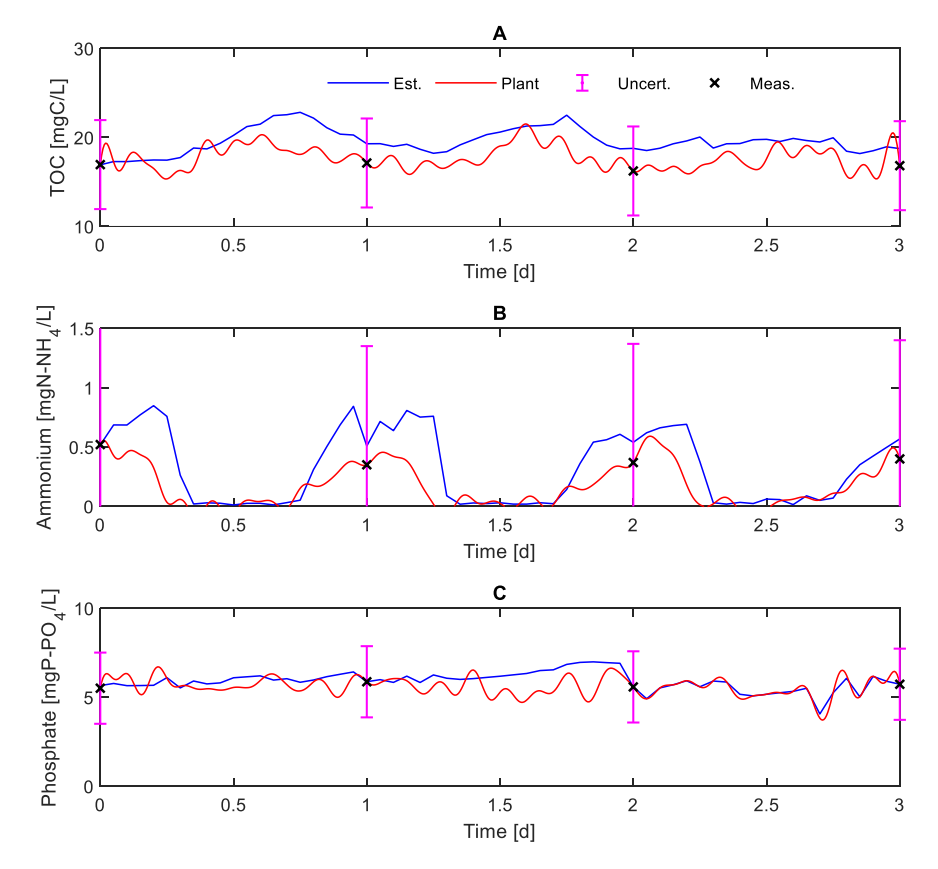


Fig. 21. Measured and estimated values of the dissolved TOC concentration (A), dissolved ammonium concentration (B), and dissolved phosphate concentration (C) under fluctuating solar radiation.

of MHE in online estimation of the most pertinent variables in the microalgae-based wastewater treatment process and its potential for future application in the development of control and optimization strategies, which requires the knowledge of system states and parameters.

CRediT authorship contribution statement

Irina Bausa-Ortiz: Writing – review & editing, Writing – original draft, Visualization, Software, Methodology, Investigation. Erika Oliveira-Silva: Writing – review & editing, Visualization, Software, Methodology. Raúl Muñoz: Writing – review & editing, Supervision, Resources. Smaranda P. Cristea: Writing – review & editing, Methodology. Cesar de Prada: Writing – review & editing, Visualization, Supervision, Resources, Methodology, Funding acquisition, Conceptualization.

Declaration of competing interest

The authors declare that they have no known competing financial interests or personal relationships that could have appeared to influence the work reported in this paper.

Acknowledgments

This research was supported by Regional Government of Castilla y León and EU-FEDER program (CL-EI-2021-07, UIC 233, UIC 379), by Regional Government of Castilla y León and the European Social Fund (Order EDU/601/2020), and by the Project a-CIDiT (PID2021-123654OB-C31).

Appendix A. Supplementary data

Supplementary data to this article can be found online at https://doi.org/10.1016/j.algal.2025.104338.

Data availability

Data will be made available on request.

References

- K.J. Chae, J. Kang, Estimating the energy independence of a municipal wastewater treatment plant incorporating green energy resources, Energ. Conver. Manage. 75 (2013) 664–672, https://doi.org/10.1016/j.enconman.2013.08.028.
- [2] R. Muñoz, B. Guieysse, Algal-bacterial processes for the treatment of hazardous contaminants: a review, Water Res. 40 (15) (2006) 2799–2815, https://doi.org/ 10.1016/j.watres.2006.06.011.
- [3] W.A.V. Stiles, et al., Using microalgae in the circular economy to valorise anaerobic digestate: challenges and opportunities, Bioresour. Technol. 267 (July) (2018) 732–742, https://doi.org/10.1016/j.biortech.2018.07.100.
- [4] S. Tebbani, F. Lopes, G. Becerra Celis, Nonlinear control of continuous cultures of Porphyridium purpureum in a photobioreactor, Chem. Eng. Sci. 123 (2015) 207–219, https://doi.org/10.1016/j.ces.2014.11.016.
- [5] J. Mohd Ali, N. Ha Hoang, M.A. Hussain, D. Dochain, Review and classification of recent observers applied in chemical process systems, Comput. Chem. Eng. 76 (2015) 27–41, https://doi.org/10.1016/j.compchemeng.2015.01.019.
- [6] D.G. Luenberger, An Introduction to Observers, IEEE Trans Automat Contr 16 (6) (1971) 596–602, https://doi.org/10.1109/TAC.1971.1099826.
- [7] D.G. Luenberger, Canonical forms for linear multivariable systems, IEEE Trans Automat Contr AC-12 (3) (1967) 290–293.
- [8] D.G. Luenberger, Observers for multivariable systems, IEEE Trans Automat Contr 11 (2) (1966) 190–197, https://doi.org/10.1109/TAC.1966.1098323.
- [9] D.G. Luenberger, Observing the state of a linear system, IEEE Transactions on Military Electronics 8 (2) (1964) 74–80, https://doi.org/10.1109/ TME 1964 4223124
- [10] R.E. Kalman, A new approach to linear filtering and prediction problems, Journal of Basic Engineering 82 (1) (1960) 35–45, https://doi.org/10.1115/1.3662552.
- [11] R.E. Kalman, R.S. Bucy, New results in linear filtering and prediction theory, J. Basic Eng. 83 (1) (1961) 95–108, https://doi.org/10.1115/1.3658902.

- [12] W.W. Su, J. Li, N.S. Xu, State and parameter estimation of microalgal photobioreactor cultures based on local irradiance measurement, J. Biotechnol. 105 (1–2) (2003) 165–178, https://doi.org/10.1016/S0168-1656(03)00188-3.
- [13] F. García-Mañas, J.L. Guzmán, M. Berenguel, F.G. Acién, Biomass estimation of an industrial raceway photobioreactor using an extended Kalman filter and a dynamic model for microalgae production, Algal Res 37 (November 2018) (2019) 103–114, https://doi.org/10.1016/j.algal.2018.11.009.
- [14] S.J. Yoo, D.H. Jeong, J.H. Kim, J.M. Lee, Optimization of microalgal photobioreactor system using model predictive control with experimental validation, Bioprocess Biosyst. Eng. 39 (8) (2016) 1235–1246, https://doi.org/ 10.1007/s00449-016-1602-0.
- [15] J.B. Rawlings, Encyclopedia of systems and control, in: Encyclopedia of Systems and Control, Springer-Verlag London, 2014, pp. 1–7, https://doi.org/10.1007/ 978-1-4471-5102-9, ch. Moving Hor.
- [16] J.B. Rawlings, B.R. Bakshi, Particle filtering and moving horizon estimation, Comput Chem Eng 30 (10–12) (2006) 1529–1541, https://doi.org/10.1016/j. compchemeng.2006.05.031.
- [17] A. Alessandri, G. Battistelli, Moving horizon estimation: Open problems, theoretical progress, and new application perspectives, Int J Adapt Control Signal Process 34 (6) (2020) 703–705, https://doi.org/10.1002/acs.3127.
- [18] S. Tebbani, L. Le Brusquet, E. Petre, D. Selisteanu, Robust moving horizon state estimation: application to bioprocesses, in: 2013 17th International Conference on System Theory, Control and Computing, ICSTCC 2013; Joint Conference of SINTES 2013, SACCS 2013, SIMSIS 2013 - Proceedings, 2013, pp. 539–544, https://doi. org/10.1109/ICSTCC.2013.6689014.
- [19] M. Elsheikh, R. Hille, A. Tatulea-Codrean, S. Krämer, A comparative review of multi-rate moving horizon estimation schemes for bioprocess applications, Comput Chem Eng 146 (2021), https://doi.org/10.1016/j.compchemeng.2020.107219.
- [20] T. Raïssi, N. Ramdani, Y. Candau, Bounded error moving horizon state estimator for non-linear continuous-time systems: Application to a bioprocess system, J. Process Control 15 (5) (2005) 537–545, https://doi.org/10.1016/j. jprocont.2004.10.002.
- [21] J. Busch, et al., State estimation for large-scale wastewater treatment plants, Water Res. 47 (13) (2013) 4774–4787, https://doi.org/10.1016/j.watres.2013.04.007.
- [22] E. Arnold, S. Dietze, Nonlinear moving horizon state estimation of an activated sludge model, IFAC Proceedings Volumes 34 (8) (2001) 545–550.

- [23] X. Yin, B. Decardi-Nelson, J. Liu, Subsystem decomposition and distributed moving horizon estimation of wastewater treatment plants, Chem. Eng. Res. Des. 134 (2013) (2018) 405–419, https://doi.org/10.1016/j.cherd.2018.04.032.
- [24] J. Abdollahi, S. Dubljevic, Lipid production optimization and optimal control of heterotrophic microalgae fed-batch bioreactor, Chem. Eng. Sci. 84 (2012) 619–627, https://doi.org/10.1016/j.ces.2012.09.005.
- [25] Metcalf & Eddy Inc., Wastewater Engineering: Treatment and Reuse, Fouth Edit, McGraw-Hill, Boston, 2003.
- [26] M. Henze, W. Gujer, M. Takashi, M. van Loosdrecht, International Water Association, Task group on mathematical modelling for design and operation of biological wastewater treatment, in: Activated sludge models ASM1, ASM2, ASM2d and ASM3, IWA Publishing, London, 2000.
- [27] A. Solimeno, C. Gómez-Serrano, F.G. Acién, BIO_ALGAE 2: improved model of microalgae and bacteria consortia for wastewater treatment, Environ. Sci. Pollut. Res. 26 (25) (2019) 25855–25868, https://doi.org/10.1007/s11356-019-05824-5.
- [28] I. Bausa-Ortiz, R. Muñoz, A.F. Torres-Franco, S.P. Cristea, C. de Prada, Parameter estimation in anoxic aerobic algal-bacterial photobioreactor devoted to carbon and nutrient removal, Algal Res. 86 (November) (2024) 2025, https://doi.org/ 10.1016/j.algal.2025.103917
- [29] A. Solimeno, L. Parker, T. Lundquist, J. García, Integral microalgae-bacteria model (BIO_ALGAE): Application to wastewater high rate algal ponds, Sci. Total Environ. 601–602 (2017) 646–657, https://doi.org/10.1016/j.scitotenv.2017.05.215.
- [30] A. Solimeno, J. García, Microalgae and bacteria dynamics in high rate algal ponds based on modelling results: long-term application of BIO_ALGAE model, Sci. Total Environ. 650 (2019) 1818–1831, https://doi.org/10.1016/j. scitotenv.2018.09.345.
- [31] F. Casagli, G. Zuccaro, O. Bernard, J.P. Steyer, E. Ficara, ALBA: a comprehensive growth model to optimize algae-bacteria wastewater treatment in raceway ponds, Water Res. 190 (2021), https://doi.org/10.1016/j.watres.2020.116734.
- [32] I. Takács, G.G. Patryioand, D. Nolasco, A dynamic model of the clarification-thickening process, Wat. Res. 25 (10) (1991) 1263–1271.
- [33] MathWorks Inc, MATLAB, 2024. R2024a.
- [34] M.J. Risbeck, J.B. Rawlings, MPCTools: Nonlinear model predictive control tools for CasADi, 2016.